

2014

Development of Visible Light-Promoted Photocatalytic O-Glycosylation, C-H Activation of Alkanes and Deoxygenation of N-(Mesyloxy) Amides

Xiaoping Wang

Louisiana State University and Agricultural and Mechanical College, xwang64@tigers.lsu.edu

Follow this and additional works at: https://digitalcommons.lsu.edu/gradschool_theses

 Part of the [Chemistry Commons](#)

Recommended Citation

Wang, Xiaoping, "Development of Visible Light-Promoted Photocatalytic O-Glycosylation, C-H Activation of Alkanes and Deoxygenation of N-(Mesyloxy) Amides" (2014). *LSU Master's Theses*. 187.
https://digitalcommons.lsu.edu/gradschool_theses/187

This Thesis is brought to you for free and open access by the Graduate School at LSU Digital Commons. It has been accepted for inclusion in LSU Master's Theses by an authorized graduate school editor of LSU Digital Commons. For more information, please contact gradetd@lsu.edu.

DEVELOPMENT OF VISIBLE LIGHT-PROMOTED PHOTOCATALYTIC *O*-
GLYCOSYLATION, C-H ACTIVATION OF ALKANES AND DEOXYGENATION
OF *N*-(MESYLOXY) AMIDES

A Thesis

Submitted to the Graduate Faculty of the
Louisiana State University and
Agricultural and Mechanical College
in partial fulfillment of the
requirements for the degree of
Master of Science

in

The Department of Chemistry

by
Xiaoping Wang
B.S., Beijing Normal University, 2011
December 2014

Acknowledgments

Firstly, I want to give thanks to my family members, who are always there to support me no matter what happens. Secondly, I really appreciate Dr. Ragains for taking me into his research group and allowing me to conduct Chemistry research in his lab. I'm really impressed by his moral personality as well as his enthusiasm for research. Through three years of graduate training under his supervision, I learned to be a critical thinker as well as researcher. Thirdly, I want to give thanks to Dr. Taylor and Dr. Zhang, my committee members. Finally, I want to take the chance to thank my current lab-mates, whom I spent my most wonderful three years of life with.

Table of Contents

Acknowledgments.....	ii
Glossary of Abbreviations.....	iv
Abstract.....	v
Chapter 1. Introduction.....	1
1.1 Photoredox Catalysis.....	1
1.2 Oligosaccharides and <i>O</i> -Glycosylation.....	2
1.3 C-H Functionalization.....	3
1.4 Amidyl Radicals.....	4
1.5 References.....	5
Chapter 2. Development of Visible Light-Promoted Photocatalytic <i>O</i> -Glycosylation.....	7
2.1 Literature Background.....	7
2.2 Original Concept of Photocatalytic <i>O</i> -Glycosylation.....	9
2.3 Results and Discussion.....	10
2.4 Experimental Section.....	18
2.5 References.....	24
Chapter 3. Development of Visible Light-Promoted Photocatalytic C-H Activation of Alkanes.....	26
3.1 Literature Background.....	26
3.2 Original Concept of Photocatalytic C-H Activation.....	27
3.3 Reagents Applied in the Photocatalytic C-H Activation.....	28
3.4 Results and Discussion.....	30
3.5 Experimental Section.....	36
3.6 References.....	38
Chapter 4. Development of Visible Light-Promoted Photocatalytic Deoxygenation of <i>N</i> -(Mesyloxy) Amide.....	40
4.1 Literature Background.....	40
4.2 Original Concept of Photoredox Catalysis to Generate Amidyl Radicals.....	42
4.3 Results and Discussion.....	44
4.4 Experimental Section.....	46
4.5 References.....	48
Vita.....	50

Glossary of Abbreviations

4 Å MS	4 Angstrom molecular sieve
Ar	Arene
Bn	Benzyl
bpy	2,2'-Bipyridine
dtbpy	4,4'-Di-tert-butyl bipyridine
DTBMP	2, 6-Di-tert-butyl-4-methylpyridine
DIPEA	Diisopropylethylamine
F-TEDA-PF ₆	1-(Chloromethyl)-4-fluoro-1, 4-diazo niabicyclo [2.2.2] octane hexafluorophosphate
HRMS	High-resolution Mass Spectrometry
LED	Light-emitting diode
m/z	Mass to charge ratio
NBS	<i>N</i> -Bromosuccinimide
NHPI	<i>N</i> -Hydroxyphthalimide
NIS	<i>N</i> -Iodosuccinimide
ppy	Phenylpyridinato
PG	Protecting group
PhSeSePh	Diphenyldiselenide
PINO	Phthalimide- <i>N</i> -oxyl radical
SCE	Saturated calomel electrode
Tf ₂ O	Trifluoromethanesulfonic anhydride
λ_{\max}	Photon absorption peak

Abstract

This thesis is divided into four chapters reporting various aspects of the background of studies and the preliminary results I obtained in three projects.

Chapter 1 gives a brief introduction to the concepts of photoredox catalysis, *O*-glycosylation, C-H functionalization and amidyl radicals.

Chapter 2 describes the development of a visible light-promoted *O*-glycosylation catalyzed by Ru(bpy)₃(PF₆)₂ or diphenyldiselenide under mild conditions. The glycosylation of primary and secondary alcohols with selenoglycosides was demonstrated with good yields, and disaccharides were constructed by coupling of the selenoglycosides in acetonitrile or dichloromethane with a glucosyl acceptor in moderate yields. The reactions catalyzed by Ru(bpy)₃(PF₆)₂ were fast and yielded moderate stereoselectivity, whereas the diphenyldiselenide-catalyzed reactions took extended time while the stereoselectivity was increased in less polar solvents. We also found that the choice of solvents had a marked effect on the stereoselectivity.

Chapter 3 introduces the development of visible light-promoted photocatalytic C-H functionalization of alkanes. Two types of C-H activation, hydroxylation and amidation of adamantane, were demonstrated in the presence of transition metal polypyridyl photocatalysts, radical precursors, and nucleophiles (H₂O or nitriles + H₂O) under blue LED irradiation. Different photocatalysts, solvents, and substrate loadings were examined to optimize the reaction conditions. Side-reactions leading to low yielding of these photocatalytic C-H functionalization reactions were also examined.

Chapter 4 discusses the importance of the amidyl radical in heterocycle construction and

remote functionalization. A novel method to produce amidyl radicals by photocatalytic reduction of *N*-mesyloxy amides was proposed. This original concept was demonstrated by the photocatalytic deoxygenation of *N*-methyl-*N*-mesyloxy-4-phenylbutyramide in the presence of 1 mol% Ir(ppy)₃ as photocatalyst, 2 equiv. diisopropylamine as terminal reducing agent and acetonitrile as solvent under blue LED irradiation. This novel method of generating amidyl radicals will be further exploited by my successor, Ms. Rashanique Quarels, to apply to heterocyclization and remote functionalization reactions.

Chapter 1. Introduction

1.1 Photoredox Catalysis

Photoredox catalysis applies the energy of light to accelerate a chemical reaction via single electron transfer processes, and has drawn the attention of the organic synthesis community due to its mildness, ease of operation, and energy-saving prospects¹⁻⁵. The most frequently applied photocatalysts are transition metal polypyridyl complexes (especially of ruthenium and iridium), like $\text{Ru}(\text{bpy})_3^{2+}$, $\text{fac-Ir}(\text{ppy})_3$, and $\text{Ir}[\text{dF}(\text{CF}_3)\text{ppy}]_2(\text{dtbbpy})^+$ (Figure 1.1)⁴.

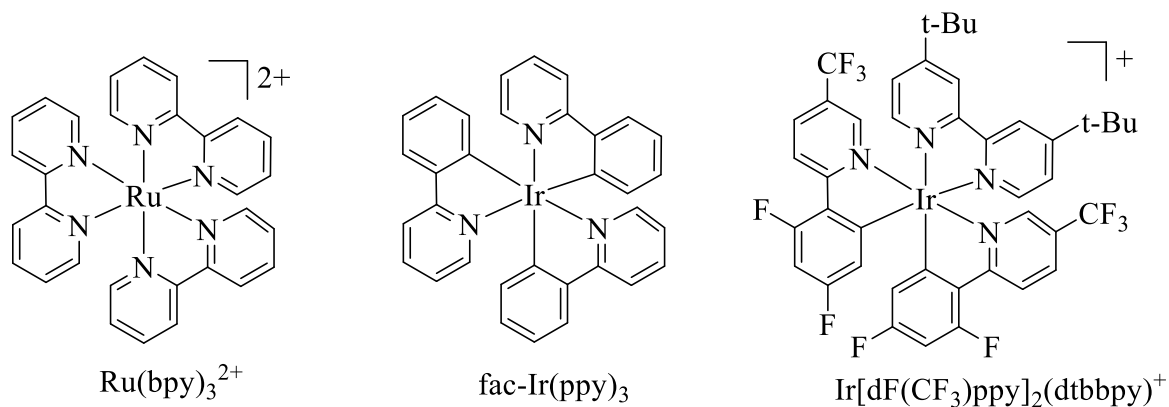


Figure 1.1: Structures of $\text{Ru}(\text{bpy})_3^{2+}$, $\text{fac-Ir}(\text{ppy})_3$ and $\text{Ir}[\text{dF}(\text{CF}_3)\text{ppy}]_2(\text{dtbbpy})^+$

Here I use $\text{Ru}(\text{bpy})_3^{2+}$ as an example to illustrate how these photocatalysts are applied in an oxidative quenching cycle and a reductive quenching cycle (Figure 1.2)⁴. Upon visible light irradiation ($\lambda_{\text{max}}=452\text{nm}$)⁴, $\text{Ru}(\text{bpy})_3^{2+}$ goes to the photoexcited state ($\text{Ru}(\text{bpy})_3^{2+*}$). The $\text{Ru}(\text{bpy})_3^{2+*}$ is an active species with low oxidation potential $\{E^0[\text{Ru}(\text{II}^*)\text{Ru}(\text{III})]=-0.81\text{ V (SCE)}\}$ ⁴, which can be oxidized easily by a mild oxidant to afford a strong oxidation reagent: $\text{Ru}(\text{bpy})_3^{3+}$ $\{E^0[\text{Ru}(\text{II})\text{Ru}(\text{III})]=+1.29\text{ V (SCE)}\}$ ⁴. The strong oxidizing reagent $\text{Ru}(\text{bpy})_3^{3+}$ can accept one electron from the material we

want to oxidize through single electron transfer, and in the process go back to the $\text{Ru}(\text{bpy})_3^{2+}$ ground state ⁴. In the reductive quenching cycle, the $\text{Ru}(\text{bpy})_3^{2+*}$ acts as milder oxidant $\{E^0[\text{Ru}(\text{I})\text{Ru}(\text{II})]=+0.77 \text{ V (SCE)}\}$ ⁴ and accepts an electron from an electron donor, which results in a strong reducing agent $\text{Ru}(\text{bpy})_3^+ \{E^0[\text{Ru}(\text{I})\text{Ru}(\text{II}^*)]=-1.33 \text{ V (SCE)}\}$ ⁴. The $\text{Ru}(\text{bpy})_3^+$ can be used to reduce the material we want to reduce and in the process go back to the $\text{Ru}(\text{bpy})_3^{2+}$ ground state ⁴.

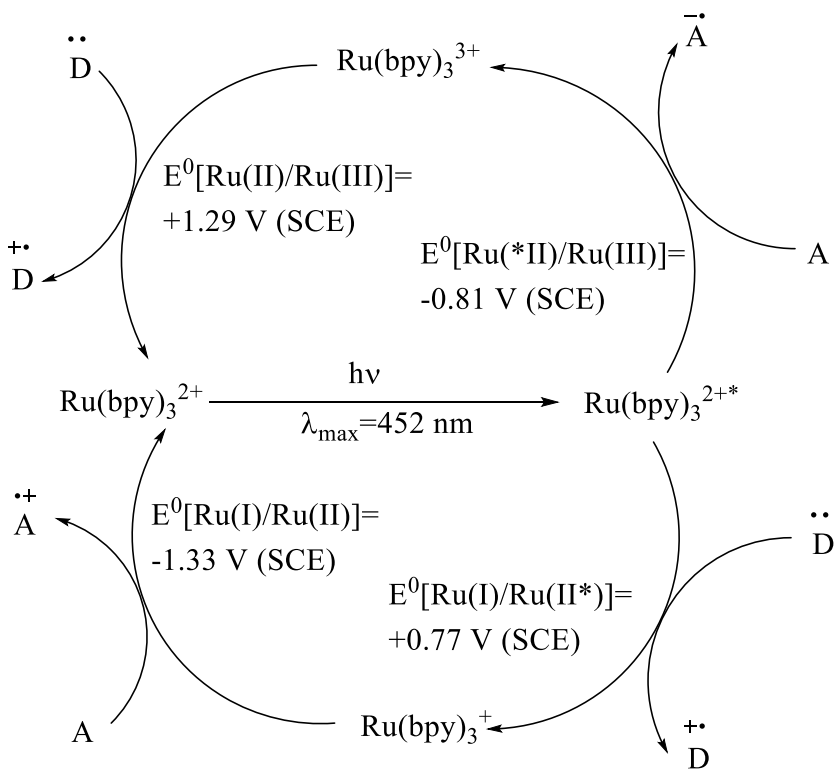


Figure 1.2: Oxidative quenching cycle (upper) and reductive quenching cycle (lower) of $\text{Ru}(\text{bpy})_3^{2+}$

1.2 Oligosaccharides and O-Glycosylation

Oligosaccharides are important in chemistry and biology because of their important roles in the structural modification of proteins, lipids, and secondary metabolites. Furthermore, they can serve as molecular recognition elements in cellular adhesion, cell-cell

recognition and cellular transport ⁶. Synthetic chemists are uniquely able to synthesize homogenous oligosaccharides as they are difficult to isolate and purify from natural sources. The central step of oligosaccharide construction is called glycosylation (Figure 1.3, using glucosides as an example) ⁷, the linking of a hemiacetal carbon of an activated carbohydrate donor (also called glycosyl donor) to a nucleophile acceptor (also called a glycosyl acceptor, often the hydroxyl group of another carbohydrate).

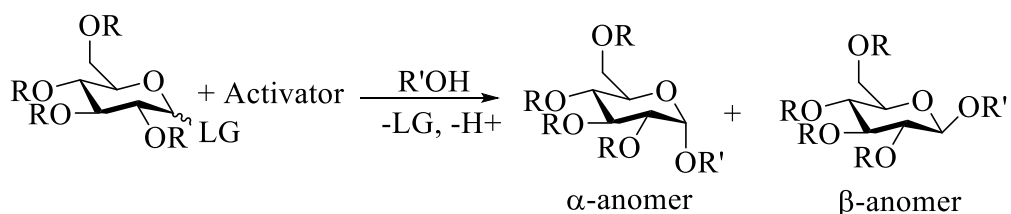
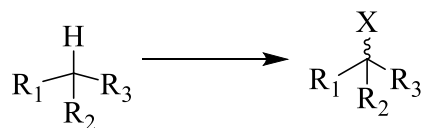


Figure 1.3: Concept for *O*-glycosylation

The glycosylated products are usually a mixture of anomers, the two stereoisomers at the hemiacetal carbon. Glycosylation has proven to be a difficult task due to the complexity of activating glycosyl donors and control of the stereochemical outcome. The traditional activation of the glycosyl donors usually requires harsh conditions or sensitive and toxic reagents. Though many glycosylation methods have been developed, none of them has yet been considered as standard ⁷⁻¹².

1.3 C-H Functionalization

C-H functionalization (Figure 1.4) is the replacement of C-H bonds (especially C-H bonds of alkanes) with C-heteroatom



X = -OH, -NHCOR, -OR, -OCOR

Figure 1.4: Concept for C-H functionalization or C-C bonds in adding a variety of functionalities like -OH, -NHCOR, -OR, and -OCOR

to hydrocarbons and natural product intermediates¹³. The direct and rapid replacement of C-H bonds with functionalities will increase the values of readily available hydrocarbons and provide advantageous strategies for the synthesis of complex molecules such as natural products. However, the inert nature of C-H bonds (not adjacent to functional groups like carbonyl) often necessitates harsh activation conditions such as the use of high temperatures and toxic or expensive reagents¹⁴.

1.4 Amidyl Radicals

Carbon-centered radicals have been widely used as intermediates in the construction of organic molecules. However, other radicals like

nitrogen-centered radicals have not received as much attention. Among the various kinds of nitrogen-centered radicals, amidyl radicals

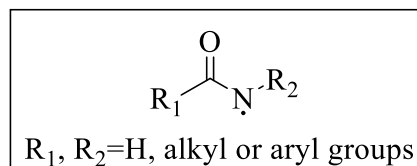


Figure 1.5: Structure of amidyl radical

(Figure 1.5) stand out because of their high electrophilicity^{15, 16}. This electrophilicity offers great potential in organic synthesis of nitrogen hetero-cycles through methods like intramolecular cyclization to afford lactams (Figure 1.6, a)¹⁵.

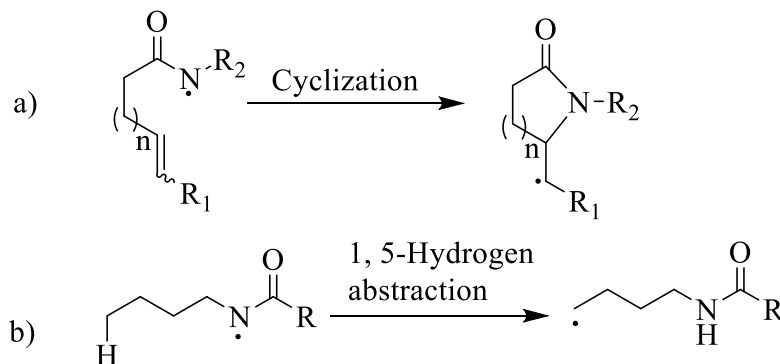


Figure 1.6: Cyclization and 1,5-hydrogen abstraction of amidyl radical

More importantly, amidyl radicals can undergo intramolecular 1, 5-hydrogen abstraction to translocate the radical to another site of the molecule, resulting in the remote functionalization of an unactivated C-H bond (Figure 1.6, b) ¹⁷.

1.5 References

1. Ischay, M. A.; Anzovino, M. E.; Du, J.; Yoon, T. P. *J. Am. Chem. Soc.* **2008**, *130*, 12886.
2. Nicewicz, D. A.; MacMillan, D. W. C. *Science*, **2008**, *322*, 73.
3. Narayanam, J. M. R.; Tucker, J. W.; Stephenson, C. R. J. *J. Am. Chem. Soc.* **2009**, *131*, 8756.
4. Prier, C. K.; Rankic, D. A.; MacMillan, D. W. C. *Chem. Rev.* **2013**, *113*, 5322.
5. Ischay, M. A.; Lu, Z.; Yoon, T. P. *J. Am. Chem. Soc.* **2010**, *132*, 8572-8574.
6. Sznajdman, M. In *Bioorganic Chemistry: Carbohydrates* (Ed.: S.M. Hecht), Oxford University Press, New York, **1999**, 1-56.
7. Koenigs, W.; Knorr, E. *Ber. Dtsch. Chem. Ges.* **1901**, *34*, 957.
8. Veeneman, G. H.; vanBoom, J. H. *Tetrahedron Letters* **1990**, *31*, 275.
9. Veeneman, G. H.; Leevwen, S. H.; Boom, J. H. *Tetrahedron Letters* **1990**, *31*, 1331.
10. Crich, D.; Sun, S. X. *J. Org. Chem.* **1997**, *62*, 1198.
11. Crich, D.; Sun, S. X. *J. Am. Chem. Soc.* **1998**, *120*, 435.
12. Nokami, T.; Shibuya, A.; Tsuyama, H.; Suga, S.; Bowers, A. A.; Crich, D.; Yoshida, J. *J. Am. Chem. Soc.* **2007**, *129*, 10922-10928.
13. Gutekunst, W. R.; Baran, P. S. *Chem. Soc. Rev.* **2011**, *40*, 1976.
14. Sakaguchi, S.; Eikawa, M.; Ishii, Y. *Tetrahedron Lett.* **1997**, *40*, 7075.
15. Chen, Q.; Shen, M. H.; Tang, Y.; Li, C. Z. *Org. Lett.* **2005**, *7*, 1625.

16. Mackiewicz, P.; Furstoss, R. *Tetrahedron* **1978**, *34*, 3241.

17. Sutcliffe, R.; Ingold, K. U. *J. Am. Chem. Soc.* **1982**, *104*, 6071.

Chapter 2. Development of Visible Light-Promoted Photocatalytic *O*-Glycosylation

2.1 Literature Background

Chalcogenoglycosides have been applied broadly as glycosyl donors because of their stability to a wide range of conditions adopted for oligosaccharide manipulation like strong Lewis acids or protic acids¹⁻⁹.

Ferrier *et al.*¹

demonstrated the first example of glycosylation utilizing

thioglycosides in 1973

(Figure 2.1, a)¹ in

which phenyl

thioglycosides were

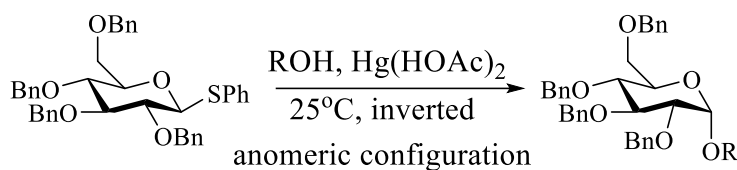
coupled with primary

or secondary alcohols

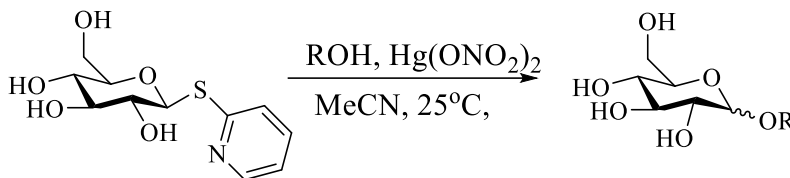
in the presence of

mercuric acetate to

a) Ferrier *et al.*



b) Hanessian *et al.*



c) Nicolaou *et al.*

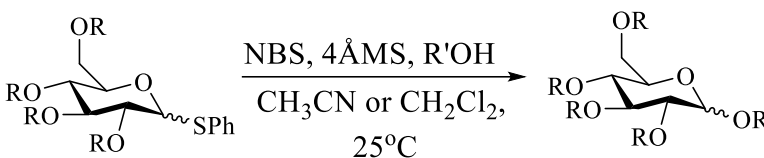


Figure 2.1: Thioglycoside *O*-glycosylation

afford *O*-alkyl glycosides with inverted anomeric configuration. Later on, this method was extended by Hanessian *et al.*² by replacing the phenyl group with other functional groups like pyridine-2-yl, pyrimidin-2-yl, and imidazolin-2-yl (the presence in the anomeric substituent of sulfur and nitrogen in a three atom arrangement could lead to remote activation) (Figure 2.1, b)², thus the activation of thioglycosides with silver or

mercury salts afforded *O*-glycoside linkages more efficiently. More recently, the Nicolaou³ group introduced another method to activate thioglycosides with NBS in the presence of alcohols to produce *O*-glycosides (Figure 2.1, c)³. Other reagents like dimethyl (methylthio) sulfoniumtriflate, iodonium dicollidine perchlorate (IDCP), NIS, Tf₂O, and PhSOTf were also reported to activate thioglycosides to afford *O*-glycosidic linkages⁴⁻⁹.

These chemical methods to activate thioglycosides suffer from drawbacks as they use harsh conditions like stoichiometric amounts of heavy metals or sensitive reagents necessitated by the stability of thioglycosides.

Electrochemical reactions are powerful tools for the activation of organic compounds without the use of highly reactive chemical reagents. Electrochemical synthetic approaches have been applied due to their selectivity, rapidity, and mild operating conditions. Electrochemical reactions involve different mechanisms than conventional chemical processes¹⁰.

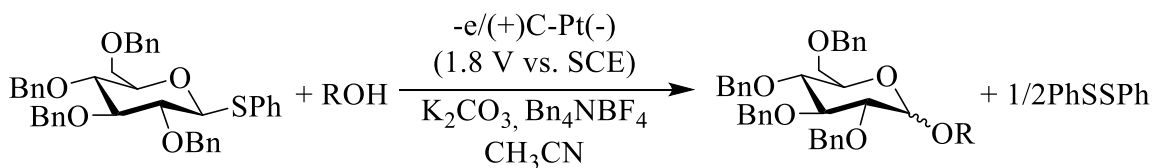


Figure 2.2: Example for electrochemical glycosylation using thioglycoside

Several groups¹¹⁻¹⁵ reported the production of glycosidic linkages through electrolysis of chalcogenoglycosides by constant current in a divided or undivided cell (example shown in Figure 2.2)¹⁰. The proposed mechanism for electrochemical glycosylation is depicted in Figure 2.3¹⁰. As shown in Figure 2.3: chalcogenoglycosides (X=S, Se) undergo anodic

oxidation to form chalcogen-centered radical cations, which quickly fragment to radicals “ArX•” and oxocarbenium ions. The oxocarbenium ions are trapped by nucleophiles (usually alcohols present in the reaction system) to afford the corresponding *O*-glycosides. Meanwhile, ArX• radicals dimerize to diaryl chalcogenides ArXXAr.

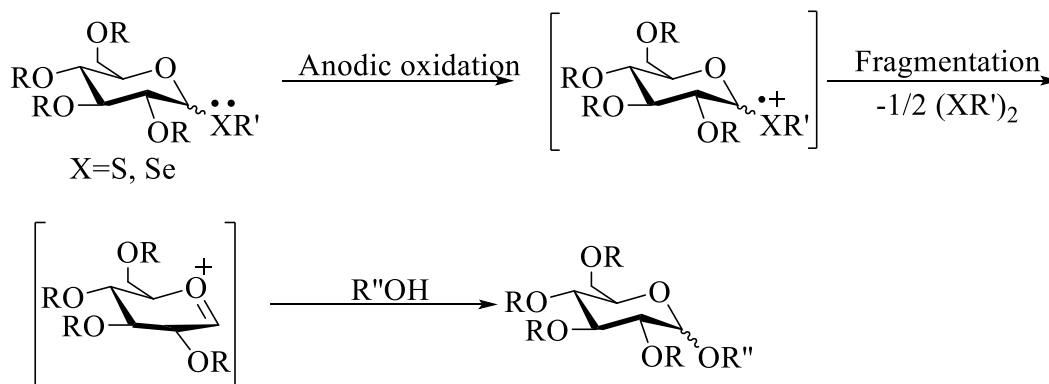


Figure 2.3: Proposed mechanism for electrochemical glycosylation

Electrochemical glycosylation is limited by the requirement of a specialized air-tight electrolysis cell. Side reactions like anodic oxidation of the resulting diaryldichalcogenide also hamper electrochemical glycosylation. Moreover, in most cases, electrochemical glycosylation provides β -linked *O*-glycosidic products predominantly¹¹⁻¹⁵. So, a general and operatively simplistic glycosylation method affording α -linked *O*-glycosides selectively using mild conditions and reagents of low toxicity is in great demand.

2.2 Original Concept of Photocatalytic *O*-Glycosylation

Based on the concept of electrochemical glycosylation, we hypothesized that $\text{Ru}(\text{bpy})_3^{3+}$ (introduced in Section 1.1, here we propose that mild oxidant CBr_4 can oxidize $\text{Ru}(\text{bpy})_3^{2+}$ to afford $\text{Ru}(\text{bpy})_3^{3+}$) can perform the same role as the anode of an

electrolysis cell to oxidize chalcogenoglycosides by single-electron transfer (Figure 2.4)^{16, 17}. The resulting radical cations of chalcogenoglycosides undergo fragmentation to form aryl chalcogeno radicals and oxocarbenium ions. The oxocarbenium ion can be trapped by glycosyl acceptors (alcohols) to afford glycosides, and aryl chalcogeno radicals dimerize to diaryl chalcogenides.

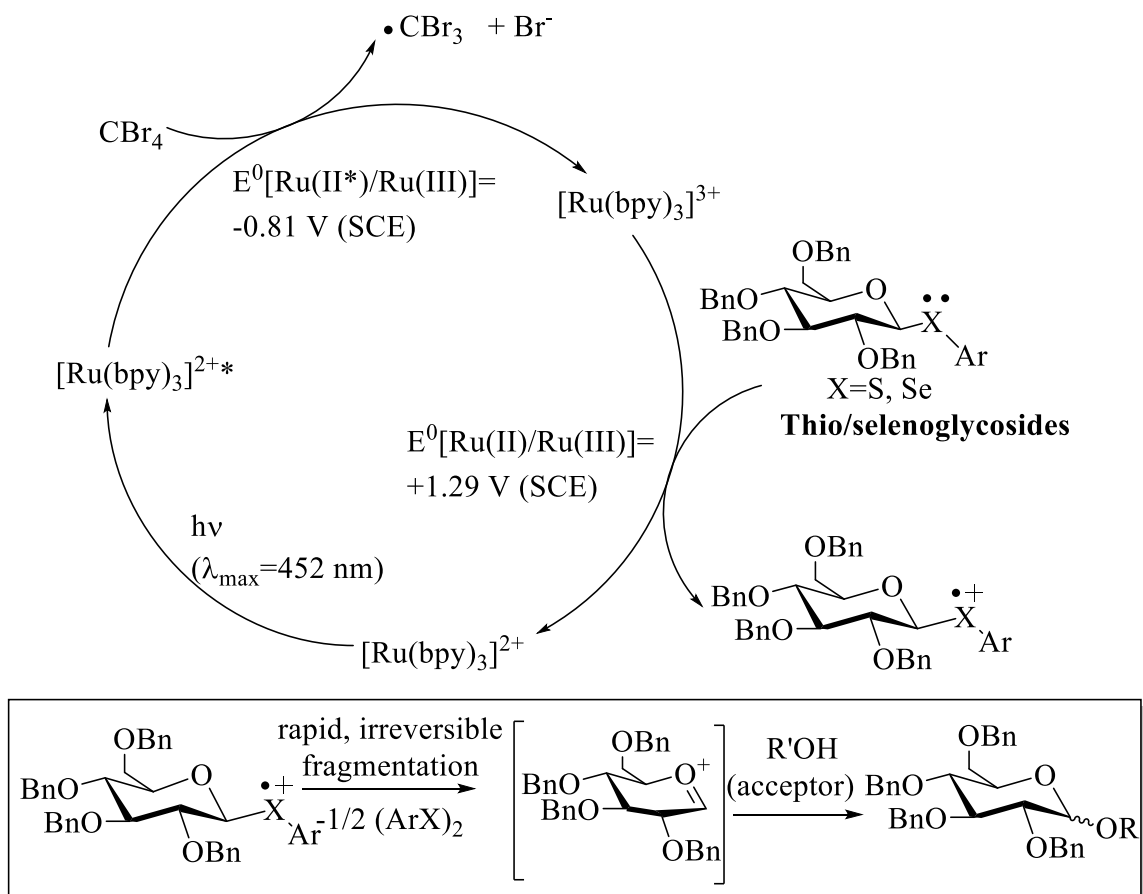


Figure 2.4: Original concept for photocatalytic *O*-glycosylation

2.3 Results and Discussion

Preparative reactions have been initiated to activate thioglycosides or selenoglycosides with $\text{Ru}(\text{bpy})_3(\text{PF}_6)_2$ as photocatalyst and a mild terminal oxidant in the presence of primary and secondary alcohols under blue LED irradiation. Previous work by my

colleague Amir Wahba demonstrated that photocatalytic glycosylation of thioglycosides (Figure 2.5) was sluggish and low yielding, so I focused on selenoglycosides as glycosyl donors as they have lower oxidation potentials compared to thioglycosides¹⁸. Investigation of

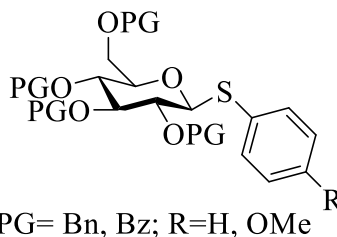


Figure 2.5 : Thioglycosides pursued in previous work

oxidants demonstrated that CBr_4 can oxidize $\text{Ru}(\text{bpy})_3^{2+*}$ to $\text{Ru}(\text{bpy})_3^{3+}$ under our photocatalytic conditions. Table 2.1 shows the results of reactions conducted. Structures of selenoglycosides, alcohols used, and glycosidic products are presented in Figure 2.6.

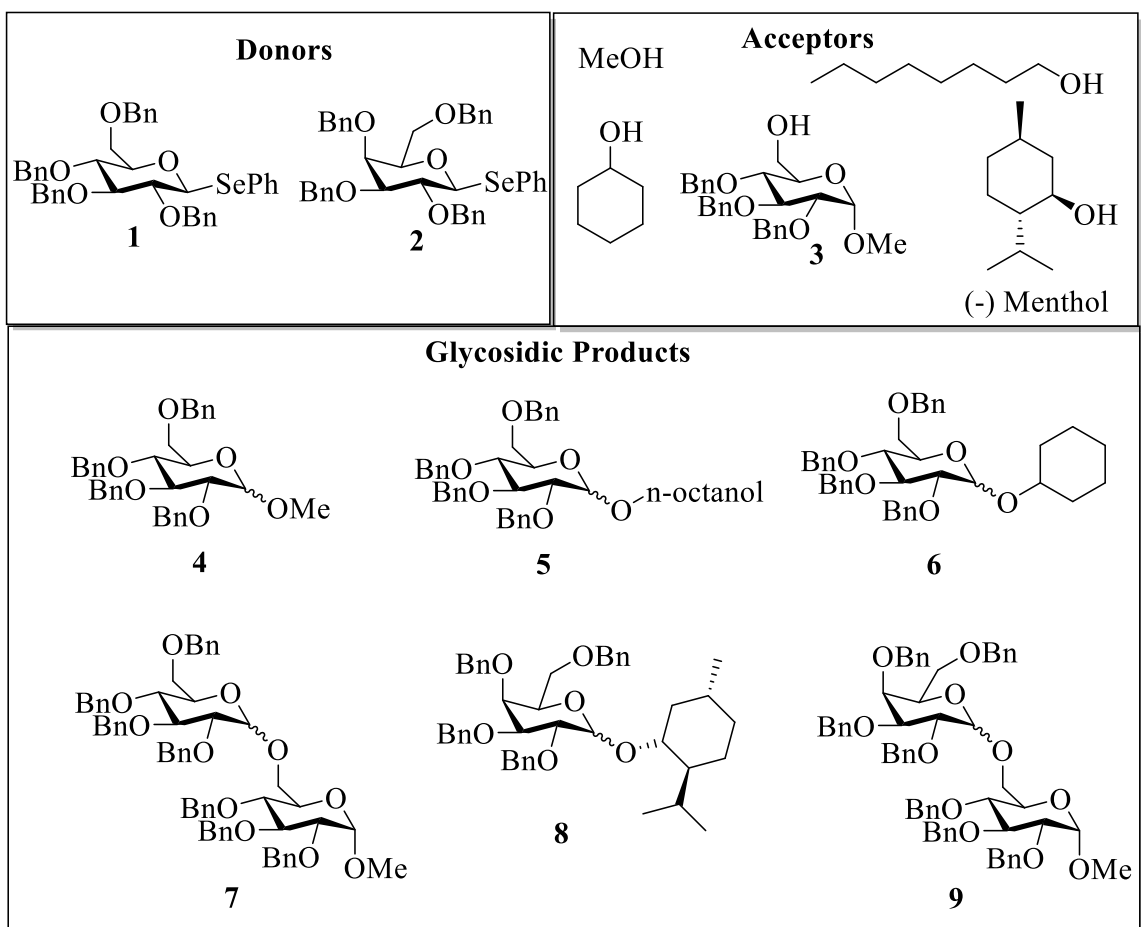
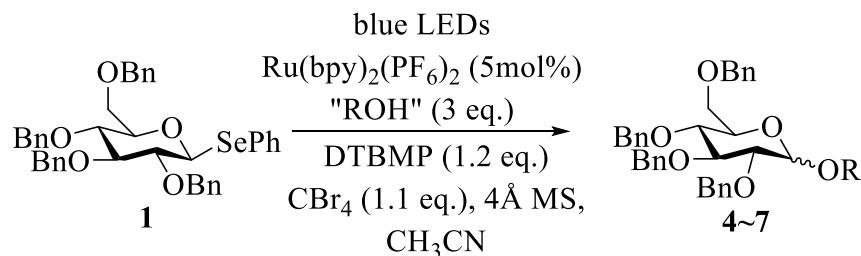


Figure 2.6: Glycosyl donors, acceptors, and glycosidic products

Table 2.1: Visible light, Ru(bpy)₃²⁺-catalyzed glycosylation



Entry	"ROH"	Irradiation time	Product	Yield (%)	Anomeric ratio (α/β)
1	MeOH	5h	4	75	2.5:1
2	1-Octanol	3h	5	81	4:1
3	Cyclohexanol	5h	6	53	8.5:1
4	3	13h	7	43	2:1
5 ^a	1-Octanol	24h	5	0	n/a
6 ^b	1-Octanol	24h	5	0	n/a
7 ^c	1-Octanol	60h	5	76	2.5:1
8 ^d	1-Octanol	18h	5	30	4:1
9 ^e	1-Octanol	5h	5	59	4:1

All experiments were performed in 5 mL Pyrex reactor vials with LED irradiation from the side (see experimental section for details). We employed 0.147 mol donor **1** with 3 equiv. alcohol acceptor, and 1.1 equiv. CBr_4 with 1.2 equiv. DTBMP in 2 mL CH_3CN . Activated 4 Å molecular sieves (400mg) were employed to dry the reaction system. Reaction mixtures characteristically reached a temperature of 40°C by adventitious heating from the LED lights. Anomeric ratios were determined by ¹H NMR analysis of purified product mixtures.

^a Performed in the absence of light

^b Performed in the absence of CBr_4

^c Performed at 50°C in the absence of light

^d Performed in the absence of $\text{Ru(bpy)}_3(\text{PF}_6)_2$

^e Performed by replacing the $\text{Ru(bpy)}_3(\text{PF}_6)_2$ with 10 mol% of diphenyldiselenide

As shown in Table 2.1 (Entry 1), 0.147 mmol of phenylseleno-2, 3, 4, 6-tetra-*O*-benzyl- β -D-glucopyranoside **1** (glycosyl donor) was activated in the presence of 5mol% Ru(bpy)₃(PF₆)₂ (photocatalyst), 1.2 equiv. DTBMP (2,6-di-*tert*-butyl-4-methylpyridine, a non-nucleophilic Bronsted base), 1.1 equiv. CBr₄ (terminal oxidant) and coupled with MeOH (3 equiv., glycosyl acceptor) to afford a 75% yield of **4** (Figure 2.4, mixture of α and β anomers) after 5 h blue LED irradiation.

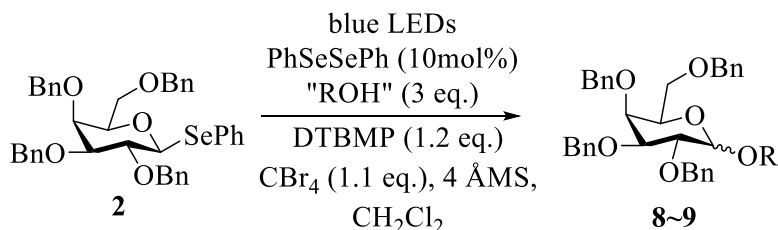
Subsequent experiments showed that this method not only promoted the coupling of selenoglucoside **1** with primary or secondary alcohols like 1-octanol (Table 2.1, Entry 2) and cyclohexanol (Entry 3) but also connected **1** with another carbohydrate acceptor **3** (Entry 4), demonstrating this method's potential for oligosaccharide synthesis. In all cases, α anomers were predominant in the product formation.

Control experiments demonstrated that light irradiation (Entry 5) and the oxidant CBr₄ (Entry 6) were necessary for this method since no conversion was observed in the absence of these two factors. Irradiation brought the reaction temperature to 40°C, so examining the thermal effect was deemed necessary. For another control (Entry 7), the reaction was heated to 50°C in the absence of light. Much slower conversion of **1** to the glycosidic products was observed by TLC and NMR (¹H NMR analysis of aliquots). A period of 60 h of heating brought this reaction to completion and afforded 76% yield of **5**. This control showed that light irradiation promotes reactions more efficiently than heating. Further, another control (Entry 8) run in the absence of Ru(bpy)₃(PF₆)₂ also resulted in complete consumption of **1** and yielded 30% of **5** as products after an extended irradiation time. This reaction drew our attention and one more experiment (Entry 9) was conducted in which Ru(bpy)₃(PF₆)₂ was replaced by 10mol% of diphenyldiselenide. In this experiment,

1 was completely consumed in only 5 h and afforded 59% of **5** with promising selectivity, which indicated that diphenyldiselenide nearly restored the reactivity of Ru(ppy)₃(PF₆)₂ in this glycosylation.

The benefits of organo-catalysis over metal-catalysis and the low cost of diphenyldiselenide (around \$10 per gram from Sigma-Aldrich) led us to further explore the diphenyldiselenide-catalyzed glycosylation. Two experiments were performed (Table 2.2) to demonstrate the concept of organo-catalytic glycosylation in collaboration with my colleague Mr. Mark Spell. Structures of glycosyl donors, acceptors and glycosidic products are listed in Figure 2.6.

Table 2.2: Visible light promoted, diphenyldiselenide-catalyzed glycosylation



Entry	"ROH"	Irradiation time	Product	Yield (%)	Anomeric ratio (α/β)
1	(-) Menthol	39h	8	55	8:1
2	3	70h	9	49	5.5:1

All experiments were performed in 5 mL Pyrex reactor vials with LEDs irradiation from the sides (see experimental section for details). We employed 0.147 mol donor **2** with 10 mol% diphenyldiselenide, 3 equiv. alcohol acceptor, and 1.1 equiv. CBr₄ with 1.2 equiv. DTBMP in 2mL CH₂Cl₂. Reaction mixtures characteristically reached a temperature of 40°C by absorbing heat from the LED lights. Anomeric ratios were determined with ¹H NMR analysis of purified product mixtures.

Hypothesizing that CH₃CN might facilitate ionization pathways that cause reduced stereoselectivity, we chose CH₂Cl₂ as a less polar solvent for the diphenyldiselenide-

catalyzed reactions. As shown in Table 2.2 (Entry 1), the galactosyl donor **2** (synthesized from commercial materials by several steps) was consumed completely after 39 h irradiation and coupled with (-) Menthol to afford **8** in a yield of 55%. This method was also effective in constructing disaccharides as shown in Table 2 (Entry 2) when **3** was applied as the glycosyl acceptor and disaccharides **9** was afforded in moderate yield.

To explore the mechanism of diphenyldiselenide-catalysis, my colleague Ms. Elizabeth Conner performed ^{77}Se NMR experiments in which a dichloromethane solution of CBr_4 and diphenyldiselenide was irradiated with blue LEDs and the formation of PhSeBr (**10**) was observed (Figure 2.6) ¹⁹.

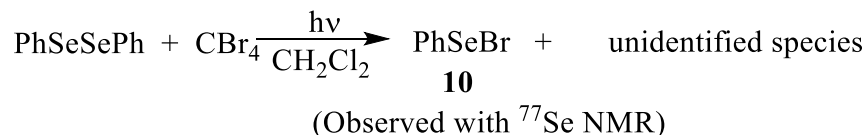


Figure 2.6: Experiments indicating the formation of PhSeBr (**10**)

We proposed a mechanism for the PhSeSePh -catalyzed glycosylation reactions as shown in Figure 2.7. Visible light promotes the homolysis of diphenyldiselenide and phenylseleno radicals are formed. The phenylseleno radicals abstract bromine atoms from CBr_4 and afford PhSeBr (**10**), which is a known electrophile ²⁰.

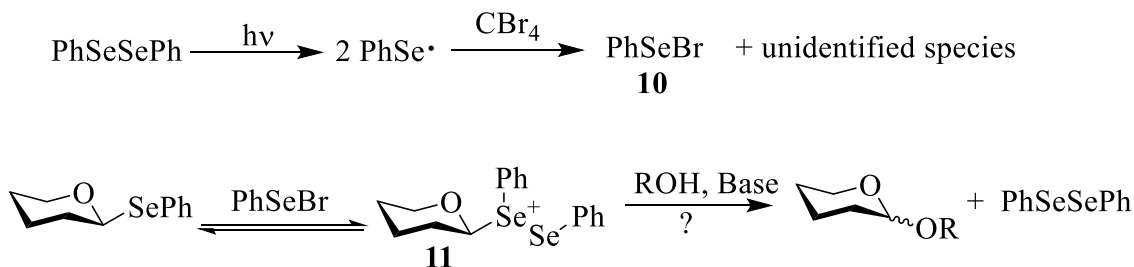


Figure 2.7: Proposed mechanism for the diphenyldiselenide-catalyzed glycosylation

The fate of CBr_4 after losing one bromine atom is uncertain. PhSeBr acts as electrophile to react with the Se atom of selenoglycoside to generate an onium species **11** and bromide. Now the question is: how does the onium species **11** proceed to the glycosidic product?

To further explore the mechanism of this photocatalytic *O*-glycosylation, Mr. Mark Spell performed control experiments in NMR tubes (Figure 2.8).

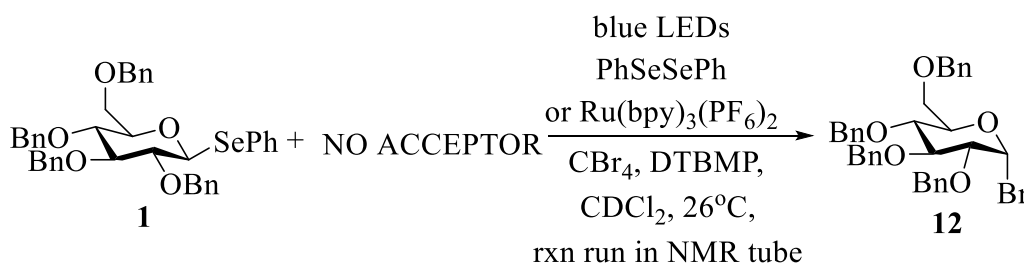


Figure 2.8: Control experiments performed in NMR tube

As shown in Figure 2.8, phenylseleno-2, 3, 4, 6-tetra-*O*-benzyl- β -D-glucopyranoside **1** was treated under our photocatalytic glycosylation conditions either using PhSeSePh or $\text{Ru}(\text{bpy})_3(\text{PF}_6)_2$ as the catalyst whereas no acceptor was added. In both cases (using 5 mol% $\text{Ru}(\text{bpy})_3(\text{PF}_6)_2$ or 10 mol% PhSeSePh as catalyst), the glucosyl donor **1** was converted to the glucosyl bromide **12** quantitatively (using 10mol% PhSeSePh as internal standard) at comparable rates in 24h according to ^1H NMR analysis. This indicated that $\text{Ru}(\text{bpy})_3(\text{PF}_6)_2$ and PhSeSePh -catalyzed glycosylations are going through the same major pathway. Moreover, Mr. Mark Spell replaced the CBr_4 in the $\text{Ru}(\text{bpy})_3(\text{PF}_6)_2$ -catalyzed glycosylation with other even stronger oxidative quenchers (Figure 2.9), it turned out that $\text{Ru}(\text{bpy})_3(\text{PF}_6)_2$ did NOT work well with them to promote the glycosylation reactions. This indicated that the single electron transfer pathway to

activate selenoglycosides (Figure 2.4, the original idea for $\text{Ru}(\text{bpy})_3(\text{PF}_6)_2$ -catalyzed glycosylation) is inefficient.

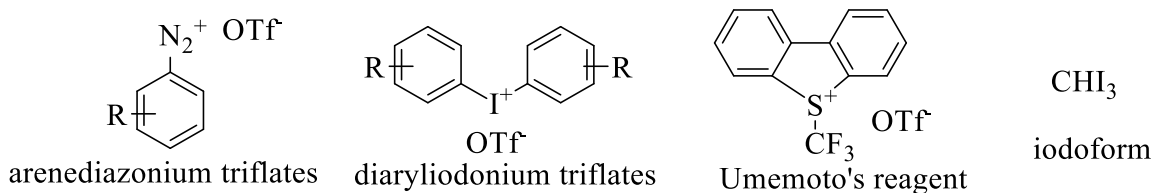


Figure 2.9: Alternative oxidative quenchers

We proposed the following mechanism for both $\text{Ru}(\text{bpy})_3(\text{PF}_6)_2$ and PhSeSePh -catalyzed glycosylation (Figure 2.10). As shown in Figure 2.10, in the first pathway, inefficient single electron transfer from the selenoglycosides to $\text{Ru}(\text{bpy})_3^{3+}$ affords the radical cations of selenoglycosides, which undergo fragmentation to form phenylseleno radicals and oxocarbenium ions.

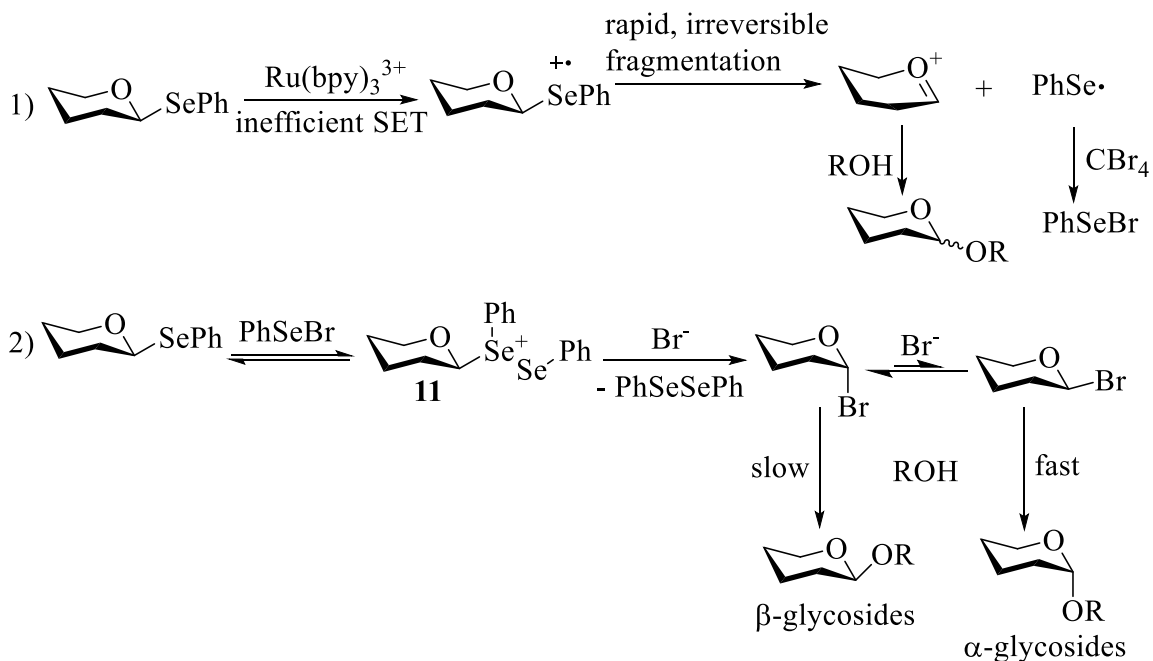


Figure 2.10: Proposed mechanism for photocatalytic *O*-glycosylation

The oxocarbenium ions can be trapped by glycosyl acceptors (alcohols) to afford glycosides (Figure 2.10, pathway 1), and phenylseleno radicals are trapped by surrounding CBr_4 to afford PhSeBr (or dimerize to PhSeSePh). As a good electrophile, PhSeBr reacts with the Se atom of selenoglycoside to generate an onium species **11** and bromide (this leads to the pathway 2 in Figure 2.10). The bromide again reacted with the onium species **11** to afford the α -glycosyl bromide, which is equilibrating to the β -glycosyl bromide. Replacing the bromide of the α -glycosyl bromide and β -glycosyl bromide afford the β - and α -glycosidic products respectively. According to Lemieux *et al.* the β -glycosyl bromide is much more reactive toward the alcohol ²¹, which explains the dominance of α -glycosidic products in our photocatalytic *O*-glycosylation.

Based on the results and mechanism studies, we proposed that in $\text{Ru}(\text{bpy})_3(\text{PF}_6)_2$ -catalyzed glycosylation, the inefficient SET pathway (Figure 2.10, pathway 1) performs as an initial as well as minor pathway to build up PhSeSePh , which sets the stage for the major pathway 2 (Figure 2.10). As for PhSeSePh -catalyzed glycosylation, the reaction will just go through pathway 2.

2.4 Experimental Section

2.4.1 General Information

Tris(bipyridyl)ruthenium(II) bis(hexafluorophosphate) ($\text{Ru}(\text{bpy})_3(\text{PF}_6)_2$) ⁵, 1-phenylselenyl-2,3,4,6-tetra-*O*-benzyl glucopyranoside ⁶ and 1-phenylselenyl-2,3,4,6-tetra-*O*-benzyl galactopyranoside ⁸ were prepared according to literatures. Flash column chromatography was performed using 60Å silica gel. ¹H NMR and ¹³C NMR spectroscopy were performed on a Bruker AV-400, DPX 400, DPX 250 or Varian 500

spectrometer. Mass spectra were obtained using an Agilent 6210 electrospray time-of-flight mass spectrometer. Optical rotation measurements were obtained using a JASCO P-2000 polarimeter. Unless otherwise noted, all materials were obtained from commercial suppliers and used without further purification. Analytical and preparative TLC were conducted on aluminum backed sheets (Merck, silica gel 60, F254). Compounds were visualized by UV absorption (254 nm) and staining with anisaldehyde. 5 mL Pyrex micro reaction vessels (Supelco) were used in the glycosylation reactions. All glassware was flame-dried under vacuum and backfilled with dry nitrogen prior to use. Deuterated solvents were obtained from Cambridge Isotope Labs. All solvents were purified according to the method of Grubbs²².

2.4.2 General procedures

a) Ru(bpy)₃(PF₆)₂-catalyzed reactions: A flame-dried 5 mL Pyrex reactor vial was charged with the glycosyl donor (1 equiv., 0.147 mmol), Ru(bpy)₃(PF₆)₂ (5 mol %, 7.4 μmol), CBr₄ (1.1 equiv., 0.161 mmol), 2,6-di-tert-butyl-4-



Figure 2.11: Experimental setup

the glycosyl acceptor (3 equiv., 0.441 mmol), 400 mg of freshly activated 4 Å molecular sieves and 2 mL of dry acetonitrile under nitrogen atmosphere. The reactor vial was placed 1-2 cm away from the light source (blue LEDs, 2 strips, Sapphire Blue LED Flex Strips from Creative Lighting Solutions, were wrapped around a 250 mL beaker, Figure 2.11) and irradiated from the side. Reaction progress was monitored by TLC. After consumption of the glycosyl donor, the reaction mixture was filtered through a silica gel

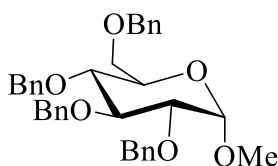
pad to remove molecular sieves and the filtrates were concentrated and then purified by gradient silica gel chromatography to afford a mixture of anomeric products.

b) PhSeSePh-catalyzed reactions: A flame dried 5 mL Pyrex reactor vial was charged with the glycosyl donor (1 equiv., 0.147 mmol), PhSeSePh (0.1 equiv., 0.014 mmol), CBr₄ (1.1 equiv., 0.161 mmol), 2,6-di-*tert*-butyl-4-methylpyridine (DTBMP) (1.2 equiv., 0.176 mmol), the glycosyl acceptor (3 equiv., 0.441 mmol), 400 mg of freshly activated 4 Å molecular sieves in 2 mL of dry CH₂Cl₂ under nitrogen atmosphere. Reaction progress was monitored by TLC. After consumption of the glycosyl donor, the reaction mixture was filtered through a silica gel pad to remove molecular sieves and the filtrates were concentrated and then purified by gradient silica gel chromatography to afford a mixture of anomeric products.

c) Determination of anomeric ratios: The anomeric ratio (α/β) was determined based on the integration of key resonances identified with the assistance of published NMR data (references provided for each compound, *vide infra*) in the ¹H-NMR of the purified anomeric mixtures. In all but one case, the major product (α -anomer) was purified by silica gel chromatography or preparative TLC.

2.4.3 Supporting information

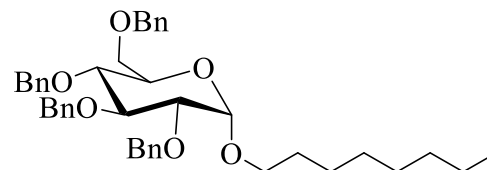
Methyl 2, 3, 4, 6-tetra-*O*-benzyl- α -D-glucofuranoside (**4**)²³:



¹H-NMR (400 MHz, CDCl₃) δ 3.37 (3H, s), 3.56 (1H, dd, $J=9.6$, 3.6 Hz), 3.62 (2H, m), 3.68-3.77 (2H, m), 3.98 (1H, t, $J=9.3$ Hz), 4.44-4.50 (2H, m), 4.57-4.69 (3H, m), 4.76-4.85 (3H, m), 4.97 (1H, d, $J=10.9$ Hz), 7.13 (2H, m), 7.23-7.38 (18H, m); ¹³C-NMR (100 MHz, CDCl₃) δ 55.2, 68.5, 70.1, 73.4, 73.5, 75.0, 75.7, 77.2, 77.7, 82.1, 98.2, 127.6, 127.7,

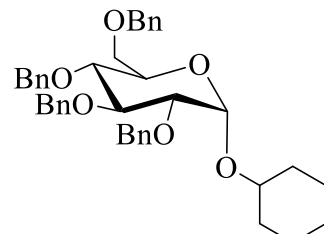
127.8, 127.9, 128.1, 128.3, 128.4, 128.5, 137.9, 138.2, 138.3, 138.8; HRMS m/z calcd for $C_{35}H_{38}KO_6$ (M+K)⁺ 593.2300, found 593.2316; $[\alpha]_D^{25} = +43.1$ ($c=0.24$, CH_2Cl_2).

***n*-Octyl 2, 3, 4, 6-tetra-*O*-benzyl- α -D-glucopyranoside (5) ¹¹:**



¹H-NMR (250 MHz, $CDCl_3$) δ 0.88 (3H, t, $J=6.8$ Hz), 1.19-1.40 (10H, m), 1.53-1.67 (2H, m), 3.40 (1H, dt, $J=9.9, 6.7$ Hz), 3.55 (1H, dd, $J=9.7, 3.5$ Hz), 3.55-3.68 (3H, m), 3.72 (1H, m), 3.78 (1H, m), 3.99 (1H, t, $J=9.2$ Hz), 4.47 (2H, d, $J=11.5$ Hz), 4.61 (1H, d, $J=12.2$ Hz), 4.64 (1H, d, $J=12.2$ Hz), 4.76 (2H, m), 4.81 (1H, d, $J=10.8$ Hz), 4.83 (1H, d, $J=10.8$ Hz), 4.99 (1H, d, $J=10.8$ Hz), 7.06-7.18 (2H, m), 7.20-7.44 (18H, m); ¹³C-NMR: (100 MHz, $CDCl_3$) δ 14.2, 22.8, 26.3, 29.4, 29.5, 29.5, 32.0, 68.4, 68.7, 70.4, 73.2, 73.6, 75.2, 75.8, 78.0, 80.3, 82.3, 97.0, 127.6, 127.8, 127.9, 128.0, 128.0, 128.1, 128.5, 128.5, 138.1, 138.4, 138.5, 139.1; HRMS m/z calcd for $C_{42}H_{52}NaO_6$ (M+Na)⁺ 675.3656, found 675.3658; $[\alpha]_D^{25} = +38.6$ ($c=0.46$, CH_2Cl_2).

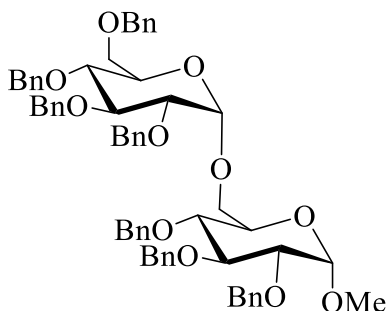
Cyclohexyl 2, 3, 4, 6-tetra-*O*-benzyl- α -D-glucopyranoside (6) ²⁴:



¹H-NMR (400 MHz, $CDCl_3$) δ 1.12-1.57 (6H, m), 1.67-1.94 (4H, m), 3.55 (2H, m), 3.63 (2H, m), 3.73 (1H, dd, $J=10.6, 3.7$ Hz), 3.88 (1H, dd, $J=10.0, 3.0$ Hz), 4.00 (1H, t, $J=9.3$ Hz), 4.47, (2H, m), 4.61 (1H, d, $J=12.2$ Hz), 4.65 (1H, d, $J=12.0$ Hz), 4.73 (1H, d, $J=12.0$ Hz), 4.82 (2H, m), 4.95 (1H, d, $J=2.8$ Hz), 4.99 (1H, d, $J=10.8$ Hz), 7.09-7.18 (2H, m), 7.22-7.40 (18, m); ¹³C-NMR (100 MHz, $CDCl_3$) δ 24.2, 24.4, 25.6, 31.4, 33.3, 68.6, 70.1, 73.0, 73.4, 75.1, 75.3, 75.6, 77.9, 80.0, 82.1, 94.7, 127.6, 127.8, 127.8, 127.9, 128.0, 128.1, 128.1, 128.2, 128.5, 128.5, 138.0, 138.3, 138.3, 139.0;

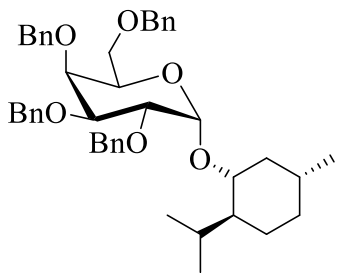
HRMS m/z calcd for $C_{40}H_{46}NaO_6$ ($M+Na$)⁺ 645.3187, found 645.3179; $[\alpha]_D^{25} = +52.7$ ($c = 0.63$, CH_2Cl_2).

Methyl-*O*-(2, 3, 4, 6-Tetra-*O*-benzyl- α -D-glucopyranosyl)-(1 \rightarrow 6)-2, 3, 4-tri-*O*-benzyl- α -D-glucopyranoside (7) ²⁵:



¹H-NMR (400 MHz, $CDCl_3$) δ 3.32 (3H, s), 3.40 (1H, dd, $J=9.6, 3.6$ Hz), 3.50 (2H, m), 3.58 (1H, t, $J=9.0$ Hz), 3.69-3.82 (3H, m), 3.87-3.99 (4H, m), 4.02 (1H, dd, $J=9.3, 3.5$ Hz), 4.36 (1H, d, $J=11.8$ Hz), 4.43 (1H, d, $J=11.9$ Hz), 4.51-4.60 (4H, m), 4.65-4.75 (4H, m), 4.75-4.82 (2H, m), 4.84 (1H, d, $J=11.0$ Hz), 4.93 (1H, d, $J=11.5$ Hz), 4.95 (1H, d, $J=10.9$ Hz), 4.99 (1H, d, $J=3.6$ Hz), 7.18-7.36 (35H, m); ¹³C-NMR (100 MHz, $CDCl_3$) δ 55.0, 66.4, 68.9, 69.4, 70.3, 72.5, 72.8, 73.3, 74.7, 75.0, 75.1, 75.7, 76.5, 77.2, 78.0, 78.3, 80.2, 82.1, 97.9, 97.9, 127.3, 127.4, 127.5, 127.6, 127.6, 127.7, 127.8, 127.9, 128.0, 128.2, 128.2, 128.2, 128.3, 128.3, 128.4, 128.4, 138.1, 138.2, 138.4, 138.7, 138.8, 138.9, 138.9; HRMS m/z calcd for $C_{62}H_{66}NaO_{11}$ ($M+Na$)⁺ 1009.4497, found 1009.4490; $[\alpha]_D^{25} = +87.2$ ($c = 0.55$, CH_2Cl_2).

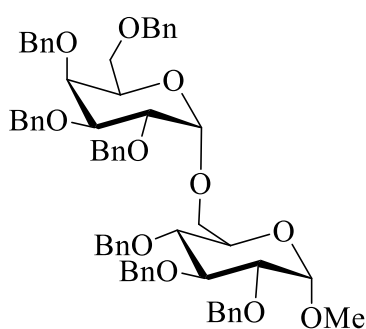
Menthyl 2, 3, 4, 6-tetra-*O*-benzyl- α -D-galactopyranoside (8) ²⁶:



¹H-NMR (500 MHz, $CDCl_3$) δ 0.69 (3H, δ , $J=6.9$ Hz), 0.81 (3H, d, $J=6.9$ Hz), 0.82 (3H, d, $J=6.0$ Hz), 0.75-0.97 (2H, m), 1.02 (1H, q, $J=12.0$ Hz), 1.20-1.40 (2H, m), 1.53-1.63 (2H, m), 2.08 (1H, d, $J=12.0$ Hz), 2.41 (1H, m), 3.33 (1H, td, $J=10.8, 4.5$ Hz), 3.54 (2H, m), 3.96 (1H, dd, $J=10.1, 2.8$ Hz), 3.99 (1H, m), 4.02 (1H, dd,

$J=10.1, 3.7$ Hz), 4.10 (1H, t, $J=9.3$ Hz), 4.42 (1H, d, $J=11.9$ Hz), 4.48 (1H, d, $J=11.9$ Hz), 4.57 (1H, d, $J=11.5$ Hz), 4.67 (1H, d, $J=11.7$ Hz), 4.74 (1H, d, $J=11.8$ Hz), 4.80 (1H, d, $J=11.5$ Hz), 4.81 (1H, d, $J=12.0$ Hz), 4.95 (1H, d, $J=11.5$ Hz), 5.02 (1H, d, $J=3.7$ Hz), 7.23-7.39 (20H, m); $^{13}\text{C-NMR}$ (125 MHz, CDCl_3) δ 16.0, 21.1, 22.3, 22.9, 24.5, 31.8, 34.3, 42.9, 48.9, 69.2, 69.3, 72.7, 73.4, 73.6, 74.7, 75.1, 79.3, 80.2, 99.3, 127.4, 127.5, 127.6, 127.7, 128.1, 128.3, 128.3, 138.1, 138.8, 138.9; HRMS m/z calcd for $\text{C}_{44}\text{H}_{54}\text{NaO}_6$ ($\text{M}+\text{Na}$) $^+$ 701.3813, found 701.3832; $[\alpha]_D^{25} = +58.3$ ($c=0.15$, CH_2Cl_2).

Methyl-*O*-(2, 3, 4, 6-tetra-*O*-benzyl- α -D-glucopyranosyl)-(1 \rightarrow 6)-2, 3, 4-tri-*O*-benzyl- α -D-galactopyranoside (9) ²⁷:



$^1\text{H-NMR}$ (400 MHz, CDCl_3) δ 3.29 (3H, s), 3.41 (1H, dd, $J=9.6, 3.6$ Hz), 3.46-3.55 (2H, m), 3.58 (1H, t, $J=9.1$ Hz), 3.63 (1H, m), 3.70-3.82 (3H, m), 3.88-4.00 (3H, m), 4.03 (1H, dd, $J=9.5, 3.5$ Hz), 4.36 (1H, d, $J=11.8$), 4.43 (1H, d, $J=11.8$ Hz), 4.52-4.61 (4H, m), 4.67-4.75 (4H, m), 4.77-4.82 (2H, m), 4.85 (1H, d, $J=11.0$ Hz), 4.93 (1H, d, $J=11.2$ Hz), 4.95 (1H, d, $J=11.2$ Hz), 4.99 (1H, d, $J=3.6$ Hz), 7.15-7.45 (35H, m); $^{13}\text{C-NMR}$ (100 MHz, CDCl_3) δ 55.0, 66.4, 68.9, 69.7, 70.5, 72.5, 72.8, 73.3, 73.5, 74.7, 75.0, 75.1, 75.7, 76.5, 78.0, 78.2, 80.2, 82.1, 97.9, 97.9, 127.5, 127.6, 127.7, 127.8, 127.8, 127.8, 127.9, 128.1, 128.3, 128.4, 128.4, 128.5, 128.5, 138.0, 138.2, 138.4, 138.7, 138.8, 138.9; HRMS m/z calcd for $\text{C}_{62}\text{H}_{66}\text{NaO}_{11}$ ($\text{M}+\text{Na}$) $^+$ 1009.4497, found 1009.4490; $[\alpha]_D^{25} = +71$. ($c=0.83$, CH_2Cl_2).

2.5 References

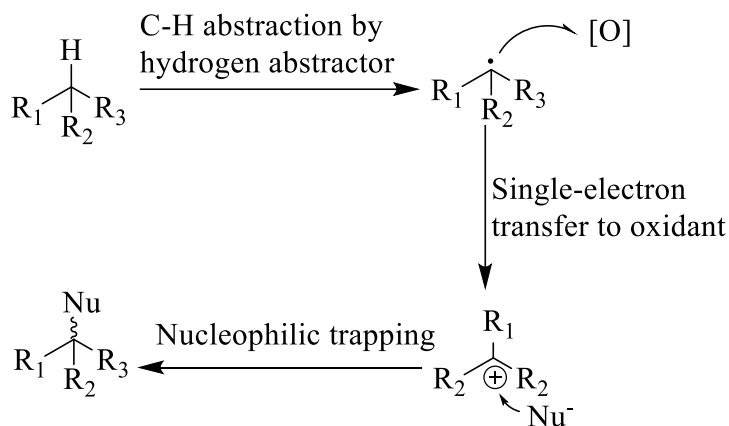
1. Ferrier, R. J.; Hay, R. W.; Vethaviasar, N. *Carbohydr. Res.* **1973**, *27*, 55.
2. Hanessian, S.; Bacouet, C.; Lehong, N. *Carbohydr. Res.* **1980**, *80*, C17.
3. Nicolaou, K. C.; Seitz, S. P. Papahatjis, D. P. *J. Am. Chem. Soc.* **1983**, *105*, 2431.
4. Anderson, F.; Fugedi, P.; Garegg, P. J.; Nashed, M. *Tetrahedron Lett.* **1986**, *27*, 399.
5. Kaahne, D.; Walker, S.; Cheng, Y.; Engen, D. V. *J. Am. Chem. Soc.* **1989**, *111*, 6881.
6. Veeneman, G. H.; Boom, J. H. *Tetrahedron Lett.* **1990**, *31*, 275.
7. Veeneman, G. H.; Leevwen, S. H.; Boom, J. H. *Tetrahedron Lett.* **1990**, *31*, 1331.
8. Crich, D.; Sun, S. X. *J. Org. Chem.* **1997**, *62*, 1198.
9. Crich, D.; Sun, S. X. *J. Am. Chem. Soc.* **1998**, *120*, 435.
10. Nokami, T.; Shibuya, A.; Tsuyama, H.; Suga, S.; Bowers, A.A.; Crich, D.; Yoshida, J. *J. Am. Chem. Soc.* **2007**, *129*, 10922-10928.
11. Nagai, H.; Sasaki, K.; Matsumura, S.; Toshima, K. *Carbohydr. Res.* **2005**, *340*, 337-353.
12. Imagawa, H.; Kinoshita, A.; Fukuyama, T.; Yamamoto, H.; Nishizawa, M. *Tetrahedron. Lett.* **2006**, *47*, 4729-4731.
13. Kumar, A.; Geng, Y.; Schmidt, R.R. *Adv. Synth. Catal.* **2012**, *354*, 1489.
14. Li, X.-B.; Ogawa, M.; Monden, T.; Maeda, T.; Yamashita, E.; Naka, M.; Matsuda, M.; Hinou, H.; Nishimura, S. I. *Angew. Chem. Int. Ed.* **2006**, *45*, 5652-5655.
15. Jona, H.; Mandai, H.; Chavasiri, W.; Takeuchi, K.; Mukaiyama, T. *Bull. Chem. Soc. Jpn.* **2002**, *75*, 291-309.
16. Nicewicz, D. A.; MacMillan, D. W. C. *Science*, **2008**, *322*, 73.
17. Prier, C. K.; Rankic, D. A.; MacMillan, D. W. C. *Chem. Rev.* **2013**, *113*, 5322.

18. Yamago, S.; Kokubo, K.; Hara, O.; Masuda, S.; Yoshida, J. *J. Org. Chem.* **2002**, *67*, 8584.
19. Conner, E.S.; Crocker, K. E.; Fernando, R. G.; Fronczek, F. R.; Stanley, G. G.; Ragains, J. *Org. Lett.* **2013**, *15*, 5558.
20. Tingoli, M.; Tiecco, M.; Testaferri, A. *J. Chem. Soc. Chem. Commun.* **1994**, 1883.
21. Lemiux, R. U.; Hendriks, K. B.; Stick, R. V.; James, K. *J. Am. Chem. Soc.* **1975**, *97*, 4056.
22. Pangborn, A. B.; Giardello, M. A.; Grubbs, R. H.; Rosen, R. K.; Timmers, F. J. *Organometallics* **1996**, *15*, 1518.
23. Potopnyk, M. A.; Cmoch, P.; Cieplak, M.; Gajewska, A.; Jarosz, S. *Tetrahedron: Asymmetry* **2011**, *22*, 780.
24. Knoblen, H. P.; Schluter, U.; Redlich, H. *Carbohydr. Res.* **2004**, *339*, 2821.
25. Dinkellaar, J.; Jong, A. R.; Meer, R.; Somers, M.; Lodder, G.; Owerkleef, H. S.; Codee, J. D. C.; Marel, G. A. *J. Org. Chem.* **2009**, *74*, 4982.
26. Tmomas, H. G.; Miesusset, J. L. *Tetrahedron* **2008**, *64*, 5124.
27. Kasprzycka, A.; Szeja, W. *Polish J. Chem.* **2005**, *79*, 329.

Chapter 3. Development of Visible Light-Promoted Photocatalytic C-H Activation of Alkanes

3.1 Literature Background

Among the strategies for C-H activation, the homolytic abstraction of hydrogen from a C-H bond to form a carbon-centered radical followed by single-electron oxidation to carbocation and then nucleophile trapping of the carbocation ¹ is very promising due to the electrophilic nature of carbocations (Figure 3.1) ¹.



Only a few examples utilizing this strategy to activate alkanes have been reported ²⁻⁵. Ishii and coworkers ³ demonstrated the amidation of adamantane using *N*-hydroxyphthalimide (NHPI) and nitric oxide (NO). The proposed mechanism is depicted in Figure 3.2 ³: phthalimide-*N*-oxyl radical (“PINO”) generated from the oxidation of *N*-hydroxyphthalimide by NO abstracts a hydrogen atom from the tertiary C-H bond of adamantane (**A**) (trace amounts of product were formed when NHPI was absent; this demonstrated that NO cannot efficiently abstract a hydrogen atom from adamantane directly). The resulting 1-adamantyl radical (**B**) is further oxidized to the adamantyl carbocation (**C**) by single-electron transfer to an electron acceptor such as NO or O₂. Nucleophilic trapping of the adamantyl carbocation (**C**) by benzonitrile and subsequent hydrolysis and tautomerization result in the formation of 1-*N*-adamantylbenzamide (**G**).

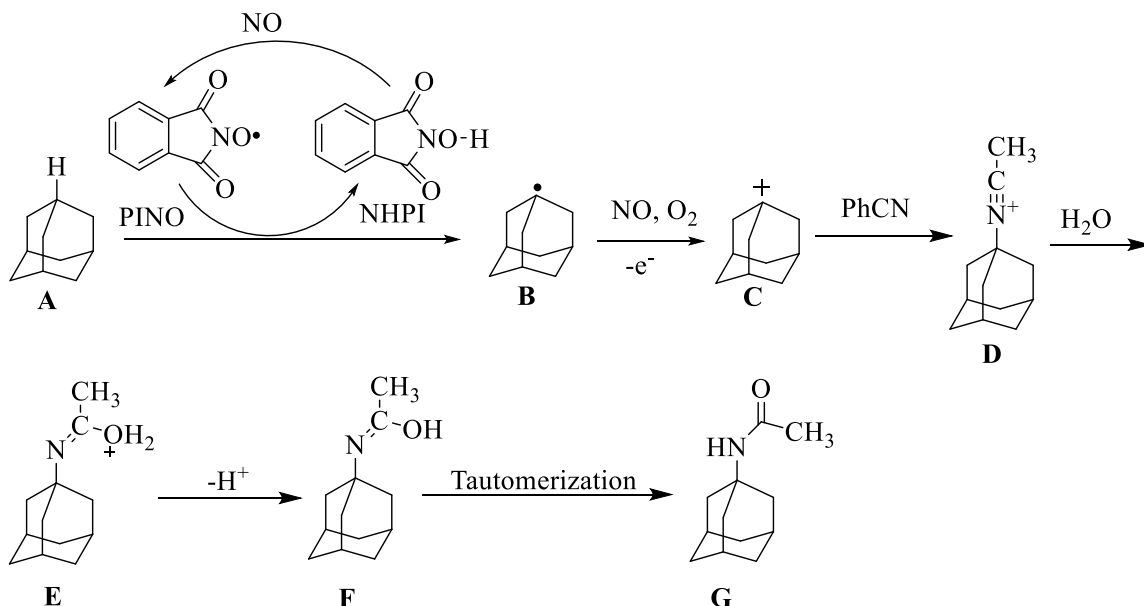


Figure 3.2: A possible mechanism for the amidation Ishii *et al.*

3.2 Original Concept of Photocatalytic C-H Activation

In this section, a visible light photocatalytic C-H activation of alkanes is proposed based on this strategy and the original concept is depicted in Figure 3.3. As shown in Figure 3.3, the photocatalytic C-H activation of alkanes requires a visible light photocatalyst (PC), a radical precursor (E-X) and a nucleophile (Nu⁻: H₂O or nitriles). The photo-excited photocatalyst PC* will reduce radical precursor (E-X) and generate electrophilic radicals (E•) that will have high reactivity and selectivity toward electron-rich C-H bonds. The carbon centered radicals generated by hydrogen abstraction of E• undergo single-electron oxidation by PC⁺ and are converted to carbocations (low concentrations of these carbon-centered radicals prevents their self-coupling). Nucleophilic trapping of the resulting carbocations leads to functionalized hydrocarbons. The regioselectivity of this method will be based on the electron density of the C-H bonds and the stability of the

resulting carbon-centered radicals (in general, tertiary C-H bonds of alkanes are more reactive towards electrophilic radicals than secondary and primary C-H bonds).

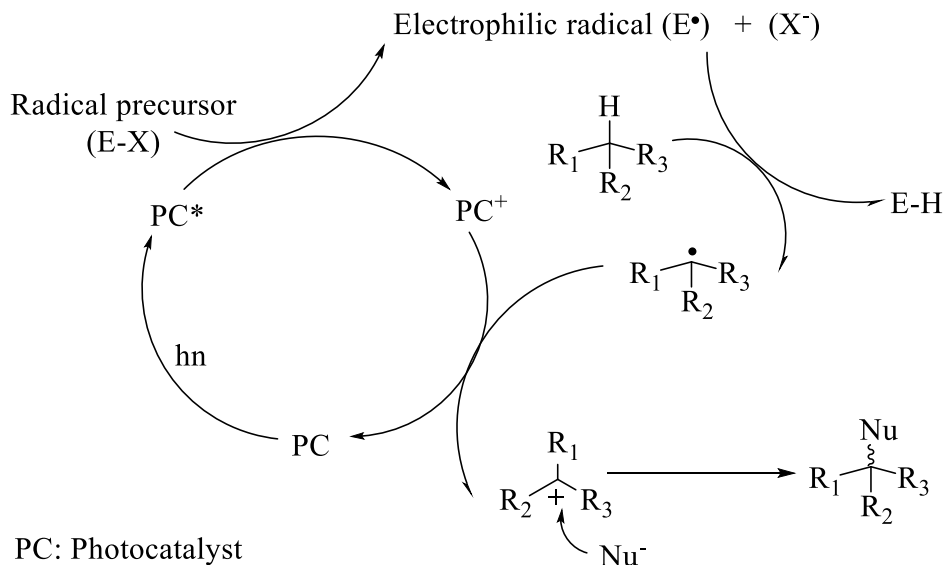
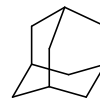


Figure 3.3 : Original concept for photocatalytic C-H activation

3.3 Reagents Applied in the Photocatalytic C-H Activation

a) Substrates and nucleophiles: Hydrocarbons with electron-rich C-H bonds are being pursued due to their reactivity and



1

selectivity toward electron-deficient hydrogen abstractors (E^\bullet). Figure 3.4: Adamantane
With a rich history in C-H functionalization³, adamantane (Figure 3.4, **1**) served as the first C-H activation substrate. Water and $\text{CH}_3\text{CN}/\text{H}_2\text{O}$ have been applied as nucleophiles to demonstrate the hydroxylation and amidation of adamantane using our photocatalytic conditions.

b) Radical precursors: Radical precursors (E-X) pursued in this method and their reduction resulting in the formation of hydrogen abstraction radicals (E^\bullet) are depicted in Figure 3.5. Trifluoromethyl radical ($\bullet\text{CF}_3$) is an electrophilic hydrogen abstractor as

demonstrated by Fuchs and coworkers ⁴. $\bullet\text{CF}_3$ can be generated effectively by single-electron reduction of Umemoto's reagent (**2**), as demonstrated by Akita and coworkers ⁵.

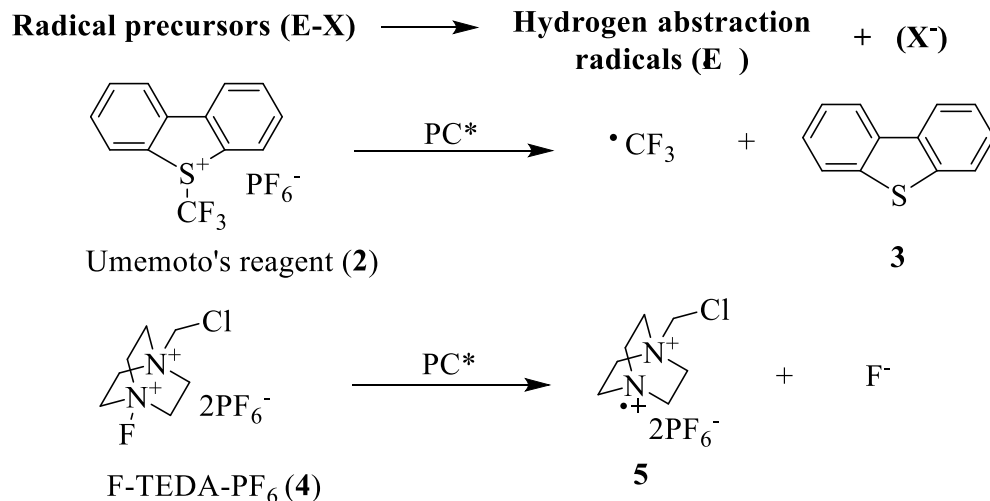


Figure 3.5: Radical precursors and radicals generated on activation species

F-TEDA-PF₆ (**4**) is another radical precursor (E-X) candidate. The high reduction potential of F-TEDA-PF₆ ($E_{1/2, \text{red, SCE}} = -0.04 \text{ V}$) ⁶ makes it easily reduced by the excited state of photocatalysts pursued in this work. As shown in Figure 3.5, we proposed that single-electron reduction of **4** would generate the radical cation **5**, which will abstract hydrogen from tertiary C-H bonds selectively.

c) Photocatalysts: Selected photocatalysts (**6**, **7**, and **8**) and their properties ⁷ are shown in Figure 3.6. In comparison, the oxidation potentials of the carbon-centered radicals ⁸ and reduction potentials of proposed radical precursors (**2** and **4**) ^{9,10} are given. As shown in Figure 3.6, the oxidation potentials [$E^0 \text{ PC/PC}^+(\text{V, SCE})$] of these excited state photocatalysts are lower than the reduction potentials [$(E_{1/2, \text{red}}(\text{V, SCE}))$] of radical precursors **2** and **4**, which will make them capable of reducing these radical precursors.

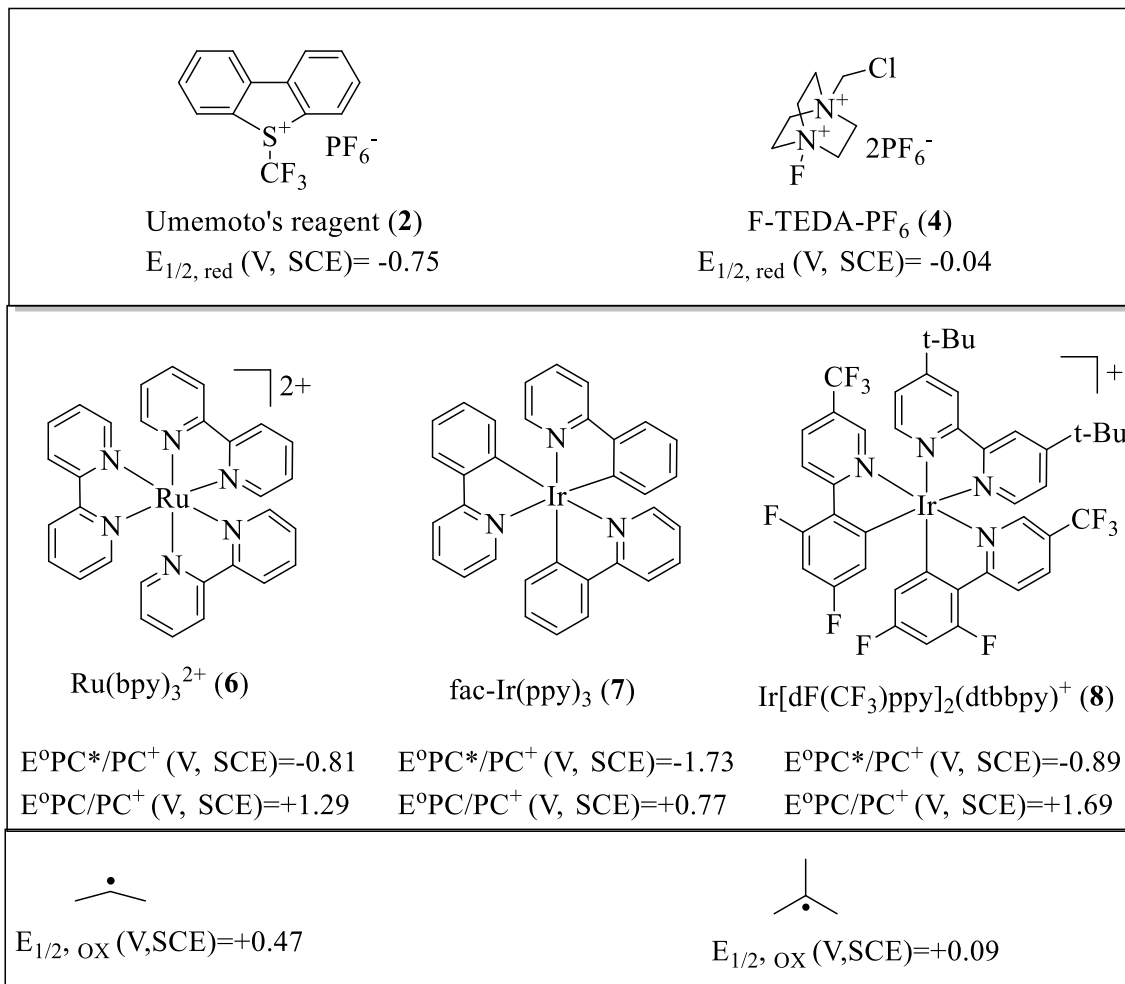


Figure 3.6: Properties of radical precursors, photocatalysts, and carbon-centered radicals

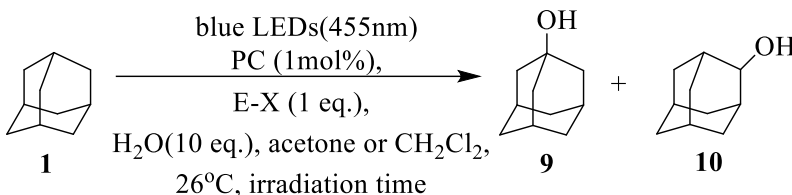
The reduction potentials of these oxidized photocatalysts are higher than the oxidation potentials of the carbon-centered radicals, so oxidation of the carbon-centered radicals to carbocations should not be a problem. For a light source, blue LEDs (~455 nm) are used to irradiate $\text{Ru}(\text{bpy})_3^{2+}$ (**6**), fac-Ir(ppy)₃ (**7**) and $\text{Ir}[\text{dF}(\text{CF}_3)\text{ppy}]_2(\text{dtbbpy})^+$ (**8**), since their absorption peaks are located around 350 to 450nm⁷.

3.4 Results and Discussion

To demonstrate the concept of photocatalytic C-H activation, preparative reactions for the hydroxylation of adamantane have been conducted applying photocatalytic conditions.

Preliminary results for the photocatalytic hydroxylation of adamantane are listed in Table 3.1.

Table 3.1: Preliminary results for photocatalytic hydroxylation of adamantane



Entry	Photocatalyst (PC)	Radical precursor (E-X)	Solvent (mL)	Irradiation time (h)	Yield (%)	Ratio (9 : 10)
1	Ru(bpy) ₃ (PF ₆) ₂ (6)	Umemoto's reagent (2)	acetone (5)	2	25	1:0
2	fac-Ir(ppy) ₃ (7)	2	acetone (5)	3	47	4:1
3	7	2	acetone (11)	17	49	2:1
4	Ir[dF(CF ₃)ppy] ₂ (dtbbpy) ⁺ (8)	2	acetone (5)	1	41	6:1
5	8	2	CH ₂ Cl ₂ (5)	0.5	37	8:1
6	6	F-TEDA-PF ₆ (4)	acetone (5)	19	15	1:0

All experiments were performed in a 25mL Schlenk flask with blue LEDs irradiation from the side (see experimental section for details). 1.25 mmol of adamantane (**1**, equiv.) was applied to react with 1 equiv. radical precursor E-X, 1mol% photocatalyst, and 10 equiv. H₂O in acetone or CH₂Cl₂. Three iterations of freeze pump thaw were applied to get rid air in the reaction system. Reactions characteristically reached a temperature of 26°C and were worked up when E-X was consumed according to TLC analysis. The two products **9**, **10** were separated by column chromatography from the crude mixture.

As shown in Table 3.1 (Entry 1), adamantane (**1**, 1.25mmol, 5 equiv.) was hydroxylated in the presence of 1mol% Ru(bpy)₃(PF₆)₂ (**6**), 1 equiv. Umemoto's reagent (**2**) and 10 equiv. of H₂O for 2h of blue LED irradiation to afford 25% of 1-adamantanol (**11**) as the product (yield based on Umemoto's reagent as limiting reagent). Subsequent experiments

(Entry 2) using another photocatalyst *fac*-Ir(ppy)₃ (**7**) afforded a higher yield (47%) with a mixture of 1-adamantanol (**9**) and 2-adamantanol (**10**) as products. The solubility of adamantane in acetone (1.25 mmol of adamantane was not completely dissolved in 5mL acetone, Entry 1 and Entry 2) was also examined to see its effect on the yielding of these reactions. In Entry 3, 11mL of acetone was applied to dissolve all the adamantane applied in the photocatalytic reactions (1.25 mmol), and this reaction afforded a mixture of products **9** and **10** with a yield of 49% after an extended time of 17 h. Because there is no significant change between Entry 3 and Entry 2, the solubility of adamantane in the reaction system might not be the primary reason for the low yield.

Ir[dF(CF₃)ppy]₂(dtbbpy)(PF₆) (**8**) was also applied to catalyze the hydroxylation of adamantane in acetone (Entry 4) or dichloromethane (Entry 5), and both reactions afforded a mixture of 1-adamantanol and 2-adamantanol with moderate yields (41% and 37%) after a short time. Side reactions of the photocatalytic hydroxylation of adamantane using Umemoto's reagent as the radical precursors were also examined. ¹H NMR, ¹³C NMR, ¹⁹F NMR, and GC/MS analysis of the crude mixtures of these reactions indicate the formation of **11**^{11, 12} and the proposed mechanism for the side reaction is shown in Figure 3.7: the •CF₃ generated from the reduction of Umemoto's reagent (**2**) by the excited state of a photocatalyst PC* adds to the dibenzothiophene **2a** to afford the radicals **2b**, which are further oxidized by the oxidized photocatalyst PC⁺ to carbocations **2c**. Finally, elimination of **2c** leads to the observed side products **11**.

In Entry 6 (Table 3.1), the hydroxylation reaction applying F-TEDA-PF₆ (**4**) as radical precursor resulted in a low yield of 1-adamantanol (15%). This reaction is still worth

investigation due to the low cost of F-TEDA-PF₆ (about \$3.0 per gram, Sigma-Aldrich) compared to Umemoto's reagent (\$91.9 per gram, Sigma-Aldrich).

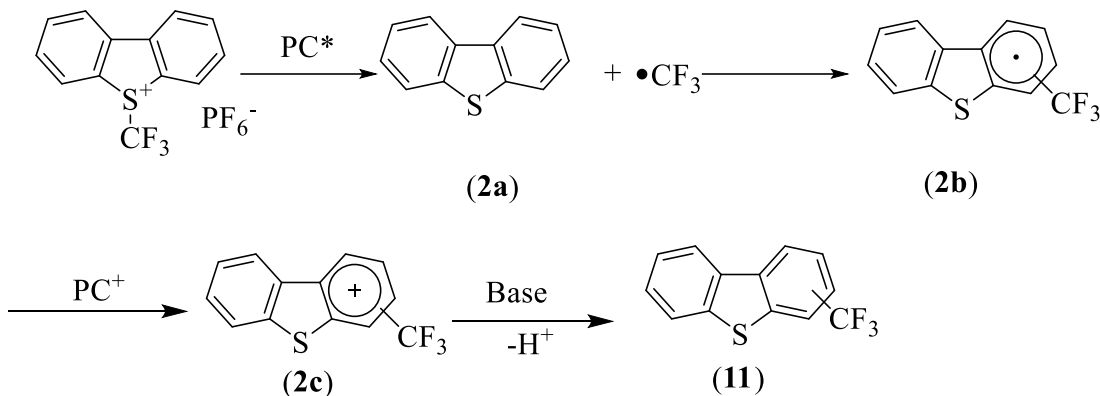


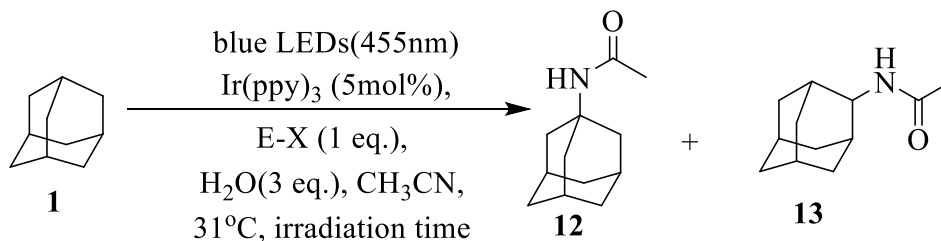
Figure 3.7: Proposed mechanism for the side reaction forming **11**

Having seen the feasibility of photocatalytic hydroxylation of adamantane (**1**), the amidation of adamantane was further demonstrated. Preparative experiments have been conducted and preliminary results are depicted in Table 3.2. As shown in Table 3.2 (Entry 1), 0.25mmol of Umemoto's reagent (**2**, 1 equiv.) was applied to react with 5 equiv. adamantane (**1**, 1.25mmol) in the presence of 5mol% fac-Ir(ppy)₃ (**7**), 3 equiv. of H₂O and the amount of CH₃CN needed to dissolve all materials. Under blue LED irradiation, these reagents underwent a Ritter reaction¹³ and the C-H bond of adamantane was functionalized resulting in formation of *N*-(1-adamantyl) acetamide (**12**) (see Figure 3.2 for the proposed mechanism of formation *N*-(1-adamantyl) acetamide from adamantyl carbocation) as product in 39% yield based on the moles of Umemoto's reagent.

To examine the effects of substrate (adamantane) loading on this reaction, in Entry 2, 1.5 equiv. adamantane (0.375 mmol) was applied to react with 1 equiv. of Umemoto's

reagent (0.25mmol) under the photocatalytic condition, and 34% yield of *N*-(1-adamantyl)acetamide (**12**) was afforded as the product after 22h irradiation.

Table 3.2: Preliminary results for photocatalytic amidation of adamantane



Entry	Radical precursor (E-X)	Equiv. of 1	Volume of CH ₃ CN (mL)	Irradiation time (h)	Yield (%)	Ratio (12 : 13)
1	Umemoto's reagent (2)	5	30	22	39	1:0
2	Umemoto's reagent (2)	1.5	9	22h	34	11:0
3	Umemoto's reagent (2)	0.8	8	17h	50	2.2:1
4	Umemoto's reagent (2)	0.5	5	17h	69	1.2:1
5	F-TEDA-PF ₆ (4)	0.5	5	26h	58	3.1:1

All experiments were performed in either a 25 or 100 mL Schlenk flask with blue LEDs irradiation from the side. 0.25mmol of radical precursor (E-X, 1 equiv.) was applied to react with adamantane (**1**, different equivalent in different entry) 5mol% photocatalyst, and 3 equiv. H₂O in the amount of CH₃CN needed to dissolve adamantane (**1**) used. Three times of freeze pump thaw was applied to get rid air in the reaction system. Reactions characteristically reached a temperature of 31°C and were worked up when the radical precursor applied was consumed according to TLC and H NMR analysis. The product **12** and **13** were separated by column chromatography from the crude mixture.

Fewer equivalents of adamantane were also applied as shown in Entry 3 and Entry 4, where 0.8 equiv. and 0.5 equiv. of adamantane were applied to react with 1 equiv. of

Umemoto's reagent, respectively. As we can see, both of these reactions afforded a mixture of *N*-(1-adamantyl)acetamide (**12**) and *N*-(2-adamantyl)acetamide (**13**) with yields of 50% and 69% respectively. This can be explained in that the $\bullet\text{CF}_3$ radical generated by the reduction of Umemoto's reagent (depicted in Figure 3.5) can either abstract a hydrogen from the tertiary or secondary carbon of adamantane (**1**), which leads to different functionalization locations on the adamantane molecule. As for the decreasing selectivity of *N*-(1-adamantyl)acetamide (**12**) over *N*-(2-adamantyl)acetamide (**13**), the reason is not clear.

Another radical precursor, F-TEDA-PF₆ (**4**) was also applied in the amidation reaction. As shown in Entry 5, 0.25mmol of F-TEDA-PF₆ (**4**, 1 equiv.) was applied to react with 0.5 equiv. adamantane (**1**, 0.125mmol) in the presence of 5 mol % *fac*-Ir(ppy)₃ (**7**), 3 equiv. of H₂O and 5ml CH₃CN. After 26h of blue LED irradiation, 58% of *N*-(1-adamantyl)acetamide (**12**) and *N*-(2-adamantyl)acetamide (**13**) was afforded. This reaction is very important because of the low cost of F-TEDA-PF₆ (**4**).

In the photocatalytic amidation of adamantane using Umemoto's reagent as the radical precursor, side products **11** were also observed in the crude reaction mixture. ¹⁹F NMR studies were also conducted to examine the possibility of $\bullet\text{CF}_3$ abstracting hydrogen atom from the solvent by running the reaction in CD₃CN, and no DCF₃ was observed by either ¹H NMR or ¹⁹F NMR. So hydrogen abstraction of $\bullet\text{CF}_3$ from solvent is not significant.

Other hydrocarbons (examples shown in Figure 3.8) were also pursued applying this photocatalytic condition, but none of them worked. Considering the limitation of this

method (works only for adamantane) and the low selectivity of products, I did not continue to optimize this method and pursued another project.

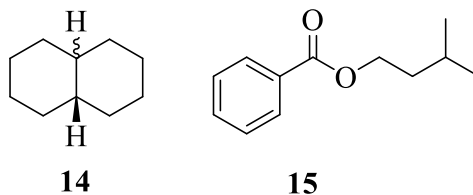


Figure 3.8: Examples of other hydrocarbons pursued

3.5 Experimental Section

3.5.1 General information

Tris[2-phenylpyridinato- C^2,N]iridium(III) [fac-Ir(ppy)₃] and 5-(trifluoromethyl)dibenzothiophenium trifluoromethanesulfonate (Umemoto's reagent) were obtained from Sigma-Aldrich. Flash column chromatography was performed using 60Å silica gel. ¹H NMR and ¹³C NMR spectroscopy were performed on a Bruker AV-400, DPX 400, DPX 250 or Varian 500 spectrometer. Unless otherwise noted, all materials were obtained from commercial suppliers and used without further purification. Analytical and preparative TLC was conducted on aluminum sheets (Merck, silica gel 60, F254). Compounds were visualized by UV absorption (254 nm) and staining with potassium permanganate solution. 25 mL (or 100mL) Schlenk flasks (Supelco) were used in the C-H activation reactions and freeze pump thaw was used. All glassware was flame-dried under vacuum and backfilled with dry nitrogen prior to use. Deuterated solvents were obtained from Cambridge Isotope Labs. All solvents were purified according to the method of Grubbs ¹⁴.

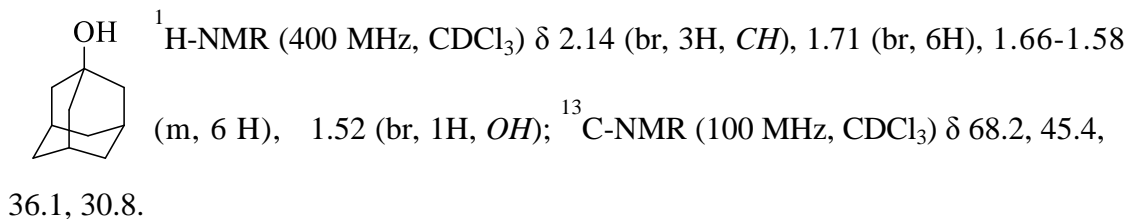
3.5.2 General procedures

a) Hydroxylation of adamantane: A 25 mL Schlenk flask was charged with adamantane (5 equiv., 1.25 mmol), radical precursor E-X (1 equiv., 0.25mmol), photocatalyst (1 mol %, 2.5 μ mol), H₂O (10 equiv., 45 μ L), 5mL acetone or CH₂Cl₂. Freeze pump thaw (three iterations) was applied to get rid of O₂ in the flask. The reaction flask was placed 1-2 cm away from the light source (blue LEDs, 2 strips, Sapphire Blue LED Flex Strips from Creative Lighting Solutions, were wrapped around a 250 mL crystallizing dish) and irradiated from the side. Reaction progress was monitored by TLC or ¹H NMR of aliquots removed from the reaction. After consumption of the radical precursor, the reaction mixture was concentrated and then purified by gradient silica gel chromatography to afford products.

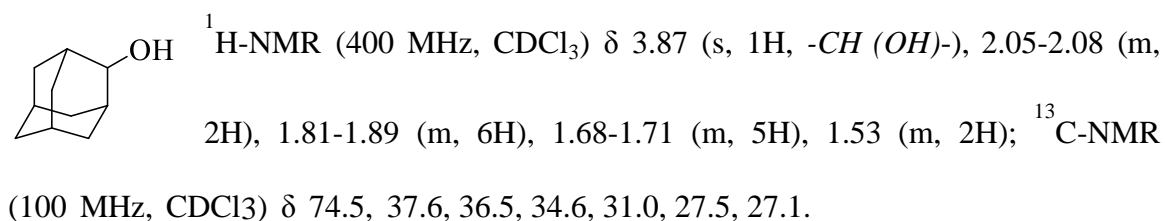
b) Amidation of adamantane: A 25 mL (or 100ml when needed) Schlenk flask was charged with adamantane (5 equiv., 1.25 mmol or less equiv.), radical precursor E-X (1 equiv., 0.25mmol), photocatalyst (5 mol %, 12.5 μ mol), H₂O (3 equiv., 15 μ L), and the quantities of CH₃CN needed to dissolve all materials (30 mL for 5 equiv. of adamantane, 9 mL for 1.5 equiv. of adamantane and so on). Freeze pump thaw (three iterations) was applied to get rid of O₂ in the flask. The reactor flask was placed 1-2 cm away from the light source (blue LEDs, 2 strips, Sapphire Blue LED Flex Strips from Creative Lighting Solutions, were wrapped around a 250 mL crystalizing dish) and irradiated from the side. Reaction progress was monitored by TLC or ¹H NMR. After consumption of the radical precursor, the reaction mixture was concentrated and then purified by gradient silica gel chromatography to afford products.

3.5.3 Supporting information

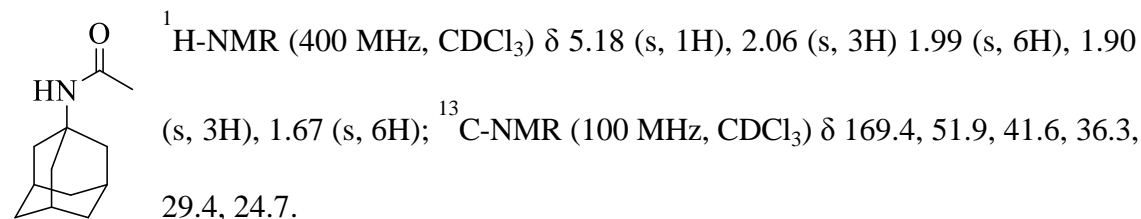
1-Adamantanol (9)¹⁵:



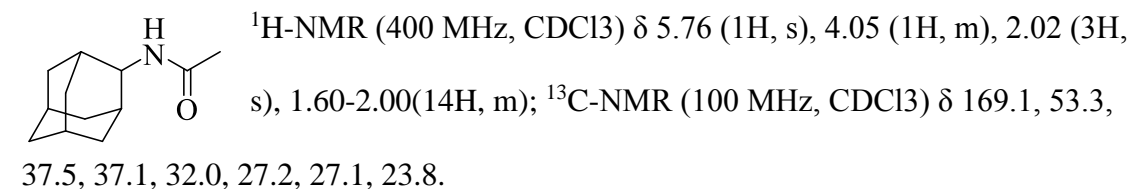
2-Adamantanol (10)¹⁶:



N-Adamantyl acetamide (12)¹⁷:



N-Adamantyl-2-acetamide (13)¹⁸



3.6 References

1. Joanna, W. D.; Thomas, D.; Fan, L.; Frank, G. *Chem. Soc. Rev.* **2011**, *40*, 4740.
2. Michaudel, Q.; Thevenet, D.; Baran, P. S. *J. Am. Chem. Soc.* **2012**, *134*, 2547.
3. Sakaguchi, S.; Eikawa, M.; Ishii, Y. *Tetrahedron Lett.* **1997**, *40*, 7075.
4. Xiang, J.; Jiang, W. L.; Gong, J. C.; Fuchs, P. L. *J. Am. Chem. Soc.* **1997**, *119*, 4123.

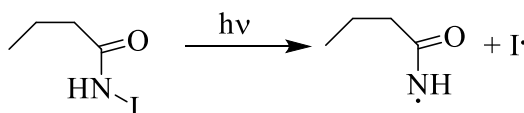
5. Yasu, Y.; Koike, T.; Akita, M. *Org. Lett.* **2013**, *15*, 2136.
6. Gilicinski, A. G.; Pez, G. P.; Syvzet, R. G.; Lal, G. S. *J. Fluorine Chem.* **1992**, *59*, 157.
7. Pier, C. K.; Rankic, D. A.; MacMillian, D. W. C. *Chem. Rev.* **2013**, *113*, 5322.
8. Ravelli, D.; Fagnoni, M. *Chem. Cat. Chem.* **2012**, *4*, 169.
9. Umemoto, T. *Chem. Rev.* **1996**, *96*, 1757.
10. Wayner, D. D. M.; Houmam, A. *Acta. Chem. Scand.* **1998**, *52*, 377.
11. Cai, J.; Wang, X. P.; Xiao, J. C.; Zhang, C. P.; Zhou, C. B.; Wang, X. P.; Zheng, X.; Gu, Y. C. *Chem. Commun.* **2011**, *47*, 9516.
12. Eisenberger, P.; Gischig, S.; Togni, A. *Chem. Eur. J.* **2006**, *12*, 2579.
13. Ritter, J. J.; Minieri, P. P. *J. Am. Chem. Soc.* **1948**, *70*, 4045.
14. Pangborn, A. B.; Giardello, M. A.; Grubbs, R. H.; Rosen, R. K.; Timmers, F. J. *Organometallics* **1996**, *15*, 1518.
15. Iwasaki, T.; Agura, K.; Maegawa, Y.; Hayashi, Y.; Mashima, K.; Ohshima, T. *Chem. Eur. J.* **2010**, *16*, 11567.
16. Battilocchio, C.; Ley, S. V.; Hawkins, J. M. *Org. Lett.* **2013**, *15*, 2278.
17. Kalkhambkar, R. G.; Waters, S. N.; Laali, K. K. *Tetrahedron Lett.* **2011**, *52*, 867.
18. Litvinas, N. D.; Brodsky, B. H.; Bois, J. D. *Angew. Chem., Int. Engl.* **2009**, *48*, 4513.

Chapter 4. Development of Visible Light-Promoted Photocatalytic Deoxygenation of *N*-(Mesyloxy) Amide

4.1 Literature Background

A number of procedures ¹⁻⁵ have been reported to generate amidyl radicals, and these procedures can be classified into two categories: fragmentation reactions and oxidation reactions. Thermal or photochemical

decomposition of haloamides (Figure 4.1)



and the fragmentation of *N'*-acyl-*N*-hydroxypyridine-2-thione carbamates ² (Figure 4.2) are representative examples for

Figure 4.1: Amidyl radicals generated by photodecomposition of iodoamides

producing amidyl radicals by fragmentation.

As shown in Figure 4.1 ¹, in the pioneering work of synthesizing lactones from amides by Barton and coworkers, it was reported that the amidyl radicals could be generated from photo-irradiation of the iodoamide ¹.

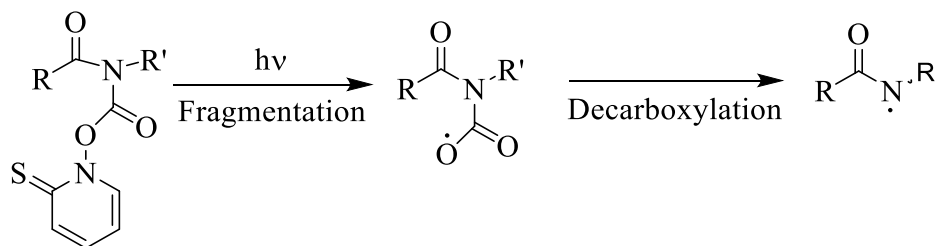


Figure 4.2. Amidyl radicals generated by fragmentation of *N'*-acyl-*N*-hydroxypyridine-2-thione carbamates

Newcomb and coworkers also reported the generation of amidyl radical by photo-initiated fragmentation of *N'*-acyl-*N*-hydroxypyridine-2-thione carbamates as shown in Figure 4.2 ². It was proposed that *N'*-acyl-*N*-hydroxypyridine-2-thione carbamates fragmented under photo-irradiation to afford the alkyl carbamoyloxy radical, which quickly underwent decarboxylation to lead to the amidyl radical. However, most of the

amidyl radical precursors are either unstable (the two amidyl radical precursors discussed above are very unstable) or difficult to prepare ³.

Li and coworkers also reported the generation of amidyl radical by thermal decomposition of relatively stable *N*-acyltriazenes ³ (Figure 4.3).

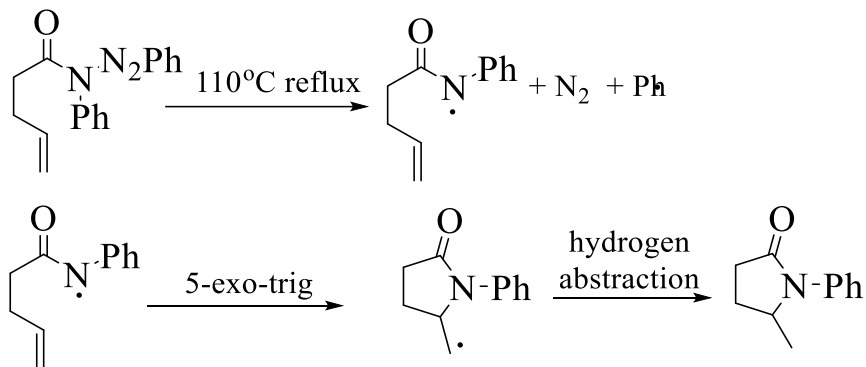


Figure 4.3: Amidyl radical generated by thermal-decomposition of triazenes

They proposed that, under refluxing benzene at 110 °C, the *N*-acyltriazenes decompose to generate the phenyl radical, nitrogen gas and the desired amidyl radical. The amidyl radical then undergoes 5-exo-trig cyclization and the resulting radical undergoes hydrogen abstraction to afford the cyclized product ³.

Another category of procedure to generate amidyl radical is by chemical oxidation of amides. In Li's work, silver-catalyzed the radical aminofluorination of unactivated alkenes in aqueous media ⁴. As shown in Figure 4.4, it was proposed that the combination of Selecfluor (1-Chloromethyl-4-fluoro-1,4-diazoniabicyclo[2.2.2]octane bis(tetrafluoroborate) and Ag(I) served to oxidize the amide by single electron transfer to afford the arene radical cations, which then undergoes deprotonation to afford the desired amidyl radical ⁴.

Later on, Moeller⁵ and coworkers also reported the cyclization reaction of anode-generated amidyl radicals, wherein they proposed the anodic oxidation of amide to afford amidyl radicals directly.

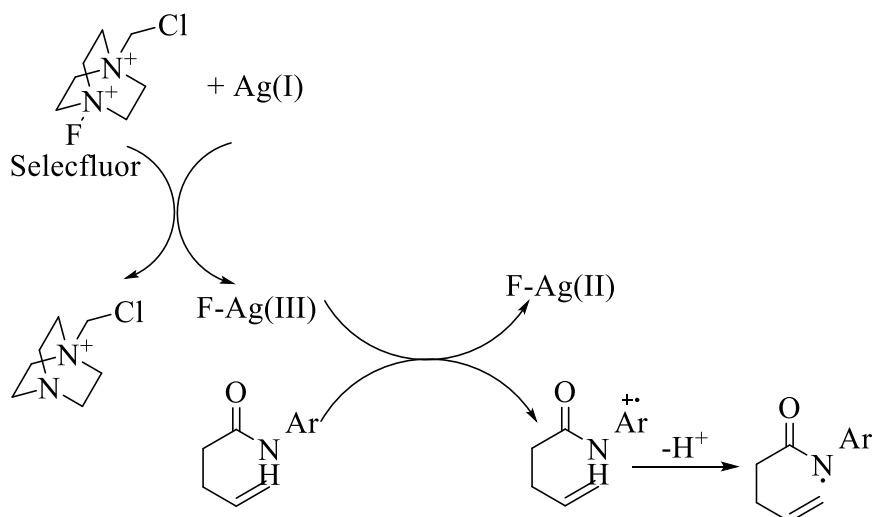


Figure 4.4: Li and coworkers proposed generation of amidyl radical by oxidation reaction

4.2 Original Concept of Photoredox Catalysis to Generate Amidyl Radicals

To broaden the application of amidyl radicals in remote functionalization or heterocyclization, the development of novel methods to generate amidyl radicals from stable radical precursors is desirable. Based on the proposed mechanism of chemical oxidation to generate amidyl radicals (Figure 4.4, the nitrogen of the amide is attached to an electron donor), we

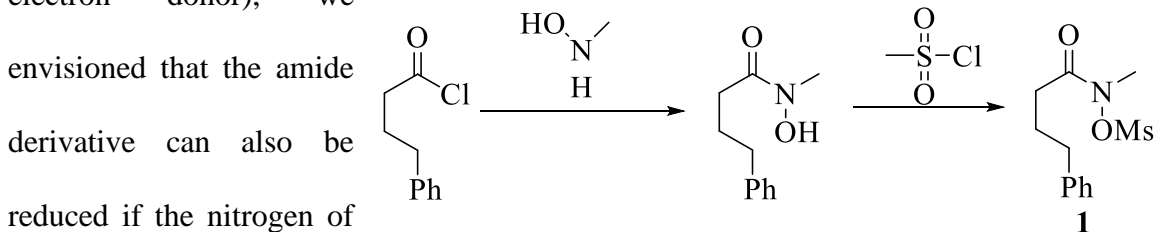


Figure 4.5: Preparation of *N*-(methoxy)amide **1**

electron acceptor as well as good leaving group such as mesylate group. To demonstrate

this concept, *N*-(methoxy)amide **1** (Figure 4.5) was prepared easily by reacting with 4-phenylbutanoyl chloride with *N*-methylhydroxylamine ⁶ and then reacting with methanesulfonyl chloride ⁷ according to literatures . We proposed that, as a good reducing reagent, photocatalyst Ir(ppy)₃ can reduce the *N*-(mesyloxy)amide **1** at its lower oxidation state by single electron transferring. Original idea proposed in Figure 4.6 ⁸.

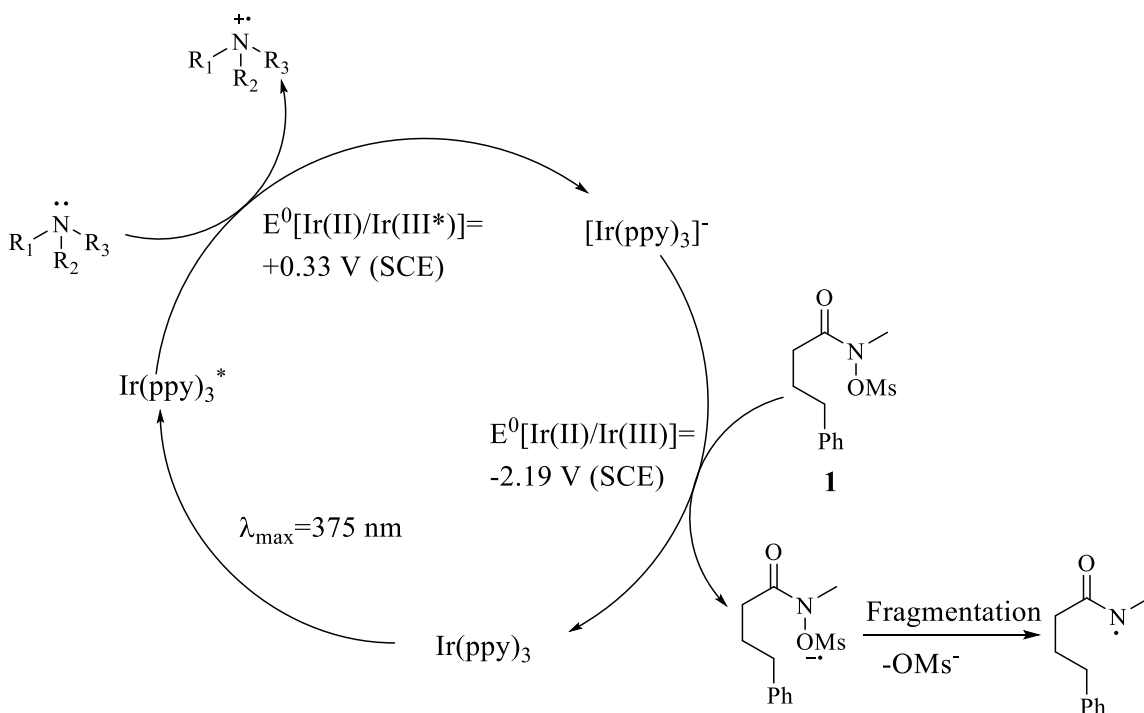


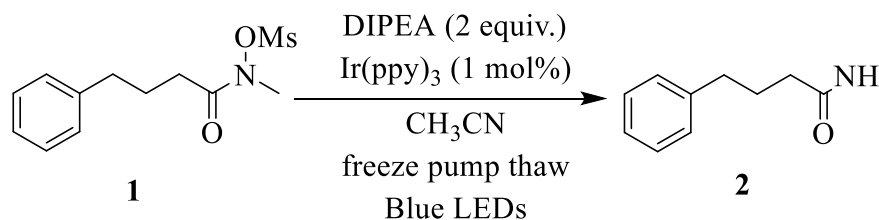
Figure 4.6: Original concept for photocatalytic reduction of *N*-(mesyloxy)amide **1** to generate amidyl radical

As proposed in Figure 4.6, the photocatalyst Ir(ppy)₃ goes to the excited state by visible light irradiation to afford Ir(ppy)₃*. The Ir(ppy)₃* is then reduced by amine to afford [Ir(ppy)₃]⁻, which serves as a great reducing agent to reduce *N*-(mesyloxy)amide **1** by single electron transfer. After receiving one electron, **1** fragmentizes to the desired amidyl radical, which undergo hydrogen abstraction or trapped by other reagent. For the fate of [Ir(ppy)₃]⁻, it will be oxidized to the ground state of Ir(ppy)₃ ⁸.

4.3 Results and Discussion

Preparative reactions have been conducted to demonstrate the original concept of photocatalytic reduction of acid derivative to generate amidyl radicals. Preliminary results are listed in Table 4.1.

Table 4.1: Visible light, Ir(ppy)₃-catalyzed deoxygenation of *N*-(mesyloxy)amide



Entry	Irradiation time	Product	Yield
1	48h	2	62%
2 ^a	48h	2	62%
3 ^b	72h	1	0
4 ^c	72h	1	0
5 ^d	72h	1	0

All experiments were performed in a 25 mL Schlenk flask with blue LEDs irradiation from the side (see experimental part for details). 0.3 mmol of the *N*-(mesyloxy)amide **1** (0.3 mmol, 1 equiv.) was applied to react with 2 equiv. diisopropylethylamine (shorted as DIPEA), 1 mol% Ir(ppy)₃, and 3 mL of CH₃CN as solvent. Three iterations of freeze pump thaw were applied to get rid of air in the reaction system. The reaction mixture characteristically reached a temperature of 26 °C and worked up when the substrate was consumed according to TLC and aqut NMR analysis. Column chromatography was applied to separate the crude reaction mixture.

^a Performed by adding 0.1 equiv of LiBF₄ was added as Lewis acid

^b Performed in the absence of Ir(ppy)₃

^c Performed in the absence of blue LEDs irradiation

^d Performed in the absence of Ir(ppy)₃ and blue LEDs irradiation

As shown in Table 4.1, 0.3 mmol (1 equiv.) of *N*-(mesyloxy) amide **1** reacted with 1 mol% of Ir(ppy)₃ as photocatalyst and 2 equiv. of diisopropylethylamine as terminal reducing

agent in the presence of blue LED irradiation to undergo the deoxygenation reaction to afford **2** as the exclusive product. In entry 2, 0.1 equiv of LiBF₄ as Lewis acid was added to the reaction mixture (we that proposed lithium ion would coordinate to the carbonyl of the substrate to reduce its reduction potential), but no change happened to the reaction time or product outcome. Control experiments (Entry 3, Entry 4, entry 5) showed that Ir(ppy)₃ and blue LEDs irradiation are necessary for the reaction to occur. Also, these control experiments demonstrated that the substrate **1** is more likely to undergo reduction reaction catalyzed by the photocatalyst instead of simple elimination promoted by diisopropylethylamine.

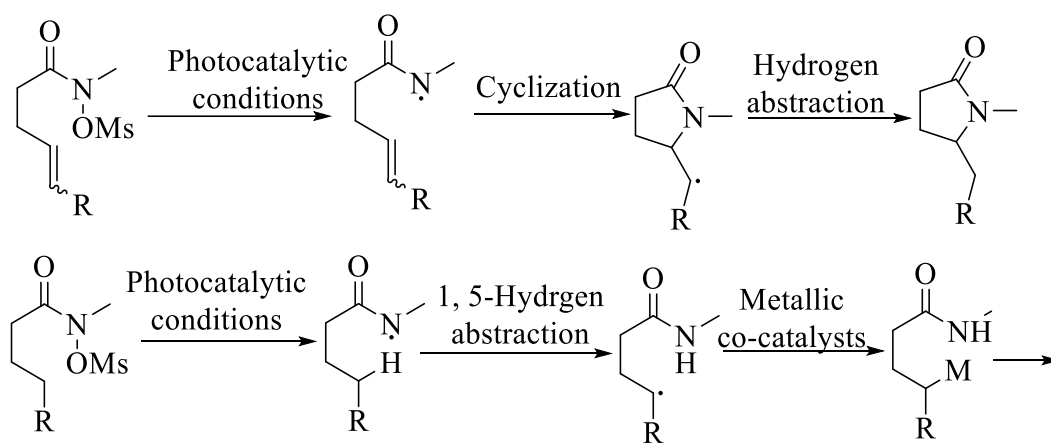


Figure 4.7: Future work applying photocatalytic reduction of *N*-(mesyloxy)amide to generate amidyl radical

The deoxygenation of *N*-(mesyloxy) amide **1** demonstrated the feasibility of generating amidyl radical by photoredox processes, which sets the stage for further application of this method to photocatalyzed amidyl radical cyclization or remote functionalization. In the future research of this project, my colleague Ms. Rashanique Quarels will adapt this method to explore lactam construction⁹ and remote functionalization¹⁰ (Figure 4.7).

4.4 Experimental Section

4.4.1 General information

Tris[2-phenylpyridinato- C^2,N]iridium(III) [*fac*-Ir(ppy)₃] was obtained from Sigma-Aldrich. Flash column chromatography was performed using 60Å silica gel. ¹H NMR and ¹³C NMR spectroscopy was performed on a Bruker AV-400, DPX 400, DPX 250 or Varian 500 spectrometer. Mass spectra were obtained using an Agilent 6210 electrospray time-of-flight mass spectrometer. Unless otherwise noted, all materials were obtained from commercial suppliers and used without further purification. Analytical and preparative TLC was conducted on aluminum sheets (Merck, silica gel 60, F254). Compounds were visualized by UV absorption (254 nm) and staining with potassium permanganate solution. 25 mL Schlenk flasks (Supelco) were used in the deoxygenation reactions and freeze pump thaw was used. All glassware was flame-dried under vacuum and backfilled with dry nitrogen prior to use. Deuterated solvents were obtained from Cambridge Isotope Labs. All solvents were purified according to the method of Grubbs ¹¹.

4.4.2 General procedure

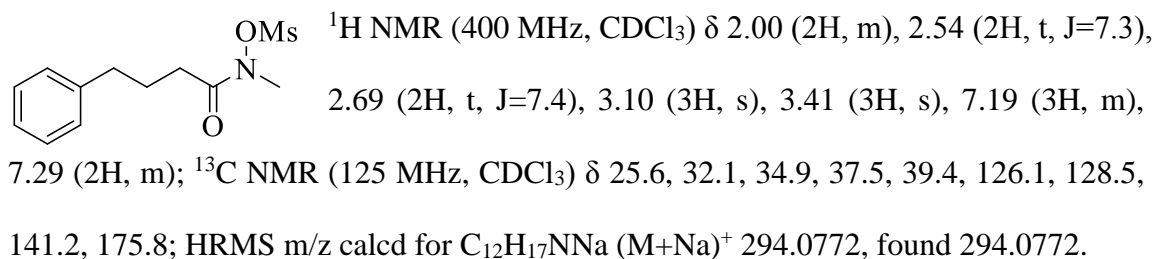
a) Preparation of *N*-methyl-*N*-mesyloxy-4-phenylbutyramide ^{6, 7}: To a solution of 4-phenylbutyric acid (6mmol) in 15 ml of dichloromethane (containing 0.1mL of dimethylformamide) was added 12 mmol of oxalyl chloride drop by drop at 0°C. The reaction was stirred at 0°C for 1 h and then concentrated. The resulting 4-phenylbutanoyl chloride was dissolved in 6mL of dry dichloromethane again and was added to a suspension of 7.2 mmol *N*-methylhydroxyamine hydrochloride containing 12 mmol triethylamine in dry dichloromethane drop by drop at 0°C. After additional stirring at 0°C

for 2 h, the mixture was washed with water (2×9mL), 1 N HCl (6mL), water (12 mL) and brine (12mL), and dried with Na₂SO₄. Filtration and evaporation of the filtrate afforded the crude mixture of the *N*-methyl-4-phenylbutarylhydroxamic acid, and no purification was applied. The *N*-methyl-4-phenylbutarylhydroxamic acid (6mmol, 1 equiv.) was redissolved in dry dichloromethane (46mL) and to this was added 1.2 equiv. of triethylamine (7.2 mmol, 1.0 mL) and 0.3 equiv. of 4-dimethylaminopyridine (1.8 mmol, 22 mg). 1.2 Equiv. of mesyl chloride (7.2 mmol, 0.56 mL) was added to the mixture dropwise at 0°C and the mixture was stirred for 0.5 h at 0°C. 0.5 N HCl was added (6mL) and the aqueous layer was extracted 3 times with of dichloromethane (12 mL). The organic extracts were combined and dried over Na₂SO₄ then filtered and concentrated. Purification of the crude mixture by chromatography afforded the *N*-methyl-*N*-mesyloxy-4-phenylbutyramide as the final product.

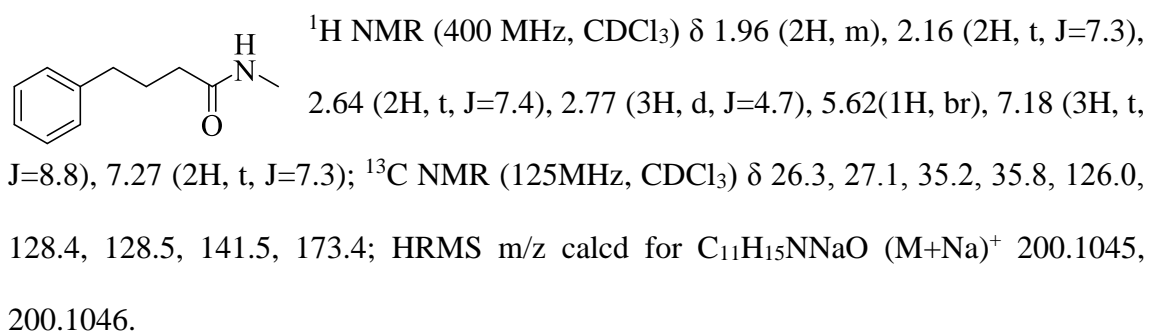
b) Deoxygenation of *N*-methyl-*N*-mesyloxy-4-phenylbutyramide: A flame dried 25 mL Schlenk flask was charged with *N*-methyl-*N*-mesyloxy-4-phenylbutyramide (1 equiv., 0.3mmol), diisopropylethylamine (2 equiv., 0.6mmol), Ir(ppy)₃ (1 mol %, 3 μmol) and 3 ml dried CH₃CN. Three iterations of freeze pump thaw were applied to get rid of O₂ in the reaction mixture. The reactor flask was placed 1-2 cm away from the light source (blue LEDs, 2 strips, Sapphire Blue LED Flex Strips from Creative Lighting Solutions, were wrapped around a 250 mL crystalizing dish) and irradiated from the side. Reaction progress was monitored by TLC or ¹H NMR. After consumption of the *N*-methyl-*N*-mesyloxy-4-phenylbutyramide as indicated by TLC analysis, the reaction mixture was concentrated and then purified by gradient silica gel chromatography to afford products.

4.4.3 Supporting information

N-Methyl-*N*-mesyloxy-4-phenylbutyramide (1)



N-Methyl-4-phenylbutyramide (2)



4.5 References

1. Barton, D. H. R.; Beckwith, A. L. J.; Goosen, A. *Photochemical Transformations. Part XVI.* **1965**, 181.
2. Esker, J.; Newcomb, M. *Tetrahedron Lett.* **1992**, 33, 5913.
3. Lu, H.; Li, C. Z. *Tetrahedron Lett.* **2005**, 46, 5983-5985.
4. Li, Z.; Song, L.; Li, C. *J. Am. Chem. Soc.* **2013**, 135, 4640-3.
5. Xu, H. C.; Campbell, J. M.; Moeller, K. D. *J. Org. Chem.* **2014**, 79, 379-91.
6. Fukuzawa, H.; Ura, Y.; Kataoka, Y. *J. Organomet. Chem.* **2011**, 696, 3643-3648.
7. Pichette, S.; Aubert-Nicol, S.; Lessard, J.; Spino, C. E. *J. Org. Chem.* **2012**, 2012, 1328-1335.
8. Prier, C. K.; Rankic, D. A.; MacMillan, D. W. *Chem. Rev.* **2013**, 113, 5322-63.
9. Esker, J.; Newcomb, M. *Tetrahedron Lett.* **1992**, 33, 5913.

10. Chen, Q.; Shen, M. H.; Tang, Y.; Li, C. Z. *Org. Lett.* **2005**, *7*, 1625.
11. Pangborn, A. B.; Giardello, M. A.; Grubbs, R. H.; Rosen, R. K.; Timmers, F. J. *Organometallic* **1996**, *15*, 1518.

Vita

Xiaoping Wang was born in Sichuan, China, to Kaiqiong Li and Ming'an Wang in 1989. He finished his high school in his hometown and went to Beijing, China for his Bachelor degree in 2007. In 2011, he was awarded with a Bachelor of Science degree at Beijing Normal University. In the same year, he came to the United States to pursue a Master of Science degree. Now he is a candidate for Master of Science in the Department of Chemistry, Louisiana State University.